Scientific Drilling
Open Access

A synthesis of monsoon exploration in the Asian marginal seas

Peter D. Clift[1], Christian Betzler[2], Steven C. Clemens[3], Beth Christensen[4], Gregor P. Eberli[5],
Christian France-Lanord[6], Stephen Gallagher[7], Ann Holbourn[8], Wolfgang Kuhnt[8],
Richard W. Murray[9], Yair Rosenthal[10], Ryuji Tada[11], and Shiming Wan[12]

[1]Department of Geology and Geophysics, Louisiana State University, Baton Rouge, LA 70803, USA
[2]Institute for Geology, German Research Fleet Coordination Center, University of Hamburg,
Bundesstrasse 55, 20146 Hamburg, Germany
[3]Department of Earth, Environmental and Planetary Sciences, Box 1846,
Brown University, Providence, RI 02912-1846, USA
[4]Department of Environmental Science, Rowan University, 201 Mullica Hill Road, Glassboro, NJ 08028, USA
[5]CSL – Center for Carbonate Research, University of Miami,
4600 Rickenbacker Causeway, Miami, FL 33149, USA
[6]Centre de Recherches Pétrographiques et Géochimiques, Université de Nancy,
CNRS UMR 7358, 54500, Vandoeuvre-lès-Nancy, France
[7]School of Geography, Earth and Atmospheric Sciences,
The University of Melbourne, Victoria, 3010, Australia
[8]Institute of Geosciences, Christian-Albrecht University, Olshausenstrasse 40, 24118 Kiel, Germany
[9]Woods Hole Oceanographic Institution, Woods Hole, MA 02543, USA
[10]School of Environmental and Biological Sciences, Rutgers, The State University of New Jersey,
71 Dudley Road, New Brunswick, NJ 08901-8520, USA
[11]Department of Earth and Planetary Science, The University of Tokyo,
7-3-1 Hongo, Bunkyo-Ku, Tokyo, 113-0033, Japan
[12]Key Laboratory of Marine Geology and Environment, Institute of Oceanology, Chinese Academy of
Sciences, 7 Nanhai Road, Qingdao, Shandong Province, 266071, China

Correspondence: Peter D. Clift (pclift@lsu.edu)

Abstract. The International Ocean Discovery Program (IODP) conducted a series of expeditions between 2013 and 2016 that were designed to address the development of monsoon climate systems in Asia and Australia. Significant progress was made in recovering Neogene sections spanning the region from the Arabian Sea to the Sea of Japan and southward to western Australia. High recovery by advanced piston corer (APC) has provided a host of semi-continuous sections that have been used to examine monsoonal evolution. Use of the half-length APC was successful in sampling sand-rich sediment in Indian Ocean submarine fans. The records show that humidity and seasonality developed diachronously across the region, although most regions show drying since the middle Miocene and especially since ~ 4 Ma, likely linked to global cooling. A transition from C_3 to C_4 vegetation often accompanied the drying but may be more linked to global cooling. Western Australia and possibly southern China diverge from the general trend in becoming wetter during the late Miocene, with the Australian monsoon being more affected by the Indonesian Throughflow, while the Asian monsoon is tied more to the rising Himalaya in South Asia and to the Tibetan Plateau in East Asia. The monsoon shows sensitivity to orbital forcing, with many regions having a weaker summer monsoon during times of northern hemispheric Glaciation. Stronger monsoons are associated with faster continental erosion but not weathering intensity, which either shows no trend or a decreasing strength since the middle Miocene in Asia. Marine productivity proxies and terrestrial chemi-

cal weathering, erosion, and vegetation proxies are often seen to diverge. Future work on the almost unknown Paleogene is needed, as well as the potential of carbonate platforms as archives of paleoceanographic conditions.

1 Introduction

Monsoon climatic systems exist in most continents where large seasonal temperature differences develop between the continental interior and the surrounding oceans. The Asian monsoon is the strongest such system because of the great size of the Asian continent and the height of the topography associated with the Himalayan mountains and Tibetan Plateau, whose development is tightly linked with the climate (Molnar et al., 1993; Prell and Kutzbach, 1992). The monsoon is split into two distinct seasons, one wet and one dry. In the summer, onshore winds bring moisture from the Bay of Bengal into South Asia and from the South China Sea and western Pacific into southern China and former Indochina (Wang, 2006; Webster et al., 1998). During northern hemispheric winter the winds reverse, with cold dry air blowing from the atmospheric high-pressure area in Siberia towards the ocean. The seasonal advance of the monsoon rain front into the continent represents a migration in the intertropical convergence zone (ITCZ) and is mirrored by a similar system that brings heavy rain to northern Australia and parts of Indonesia during the southern hemispheric summer (Suppiah, 1992).

There has been significant scientific interest in monsoon climates because the Asian monsoon has come to symbolize the archetypal example of how the solid Earth and atmosphere coevolve, with feedbacks between the two over various timescales (Clift et al., 2008; Whipple, 2009). The societal significance of the Asian monsoon has also made it the target of research given the high population density that is sustained by the agriculture permitted by summer rainfall today, as well as its role in controlling the rise and subsequent decline of early urban civilizations (Madella and Fuller, 2006; Clift and d'Alpoim Guedes, 2021). Although much is known about the atmospheric physics that controls the intensity of the monsoon in the present day, the long-term development of this climatic system is less well characterized, especially prior to the Quaternary.

Scientific drilling in the 1980s played a crucial role in the first attempt to constrain the timing of Asian monsoon intensification, particularly through records of oceanic upwelling and productivity along the Arabian margin (Kroon et al., 1991; Prell et al., 1992), where strong summer winds are linked to the monsoon in the present day. The winds blow to the northeast offshore Arabia, bringing nutrient-rich water to the surface that causes a seasonal bloom in planktic foraminifers in the modern Arabian Sea during the summer (Curry et al., 1992). In turn an oxygen minimum zone (OMZ) forms in response to the high marine productivity driven by monsoon-induced upwelling (Altabet et al., 1995) and because of limited vertical mixing. This phenomenon is particularly well developed along the NE margin offshore India and Pakistan. The OMZ is greater when the productivity is high and when winter mixing of the water column is shallow (Reichart et al., 1998). Correlation of these records with terrestrial vegetation proxies in the Himalayan foreland basin played a key role in leading to an estimate for initial intensification at ~ 8 Ma (Quade et al., 1989), which at that time was believed to correlate with a phase of rapid Tibetan uplift (Harrison et al., 1992). Subsequently, re-examination of the Oman margin cores has resulted in recognition of an initial monsoon wind system starting at 12.9 Ma and intensifying ~ 7 Ma (Gupta et al., 2015). Drilling in the South China Sea by the Ocean Drilling Program (ODP) Leg 184 in 1999 established a contrasting chemical weathering and salinity record that implied a much earlier intensification of heavy rains in southern China, starting around 24 Ma and again at 15 Ma (Clift et al., 2002; Wan et al., 2007) and indicated a drying of the climate in the late Miocene (Steinke et al., 2010).

It is apparent that a number of different processes control the strength of the monsoon systems by influencing the temperature of the continent as well as the oceans. In particular, the development of high topography in central Asia has been invoked to cause long-term strengthening of the monsoon system, and while early efforts focused mostly on the Tibetan Plateau (Manabe and Terpstra, 1974), greater emphasis has recently been placed on the height of the Himalayas and their role in controlling the South if not East Asian monsoon (EAM) (Boos and Kuang, 2010). Climate models have, however, also invoked the importance of topography in the Iranian Plateau (Acosta and Huber, 2020), as well as the opening and closure of marine gateways, most notably in the western Tethys Ocean between Arabia and Eurasia (Gülyüz et al., 2020; Torfstein and Steinberg, 2020). In addition, constriction of the Indonesian Throughflow (ITF), the oceanic gateway between Indian and Pacific oceans, has increased as Australia collided with Indonesia and New Guinea starting in the Miocene (Van Ufford and Cloos, 2005). Added to this, it has become apparent that the monsoon rainfall is sensitive to global climate in being generally heavier when Earth is hotter. On shorter glacial–interglacial timescales, it has been recognized that monsoon rains tend to be stronger during interglacial times in Asia and become drier during periods of extensive northern hemispheric glaciation. Multi-proxy reconstructions from recent drilling indicate that coupled ice volume and greenhouse gas forcing is a critical factor driving changes in monsoonal rainfall at orbital timescales as well (Clemens et al., 2021; Gebregiorgis et al., 2018; McGrath et

al., 2021). On shorter timescales oceanic phenomena such as the El Niño–Southern Oscillation (ENSO) are often linked to the strength of monsoon rains in Asia (Wang et al., 2013; Lau and Wang, 2006).

The Australian monsoon is linked to the Asian system but has different sensitivities. A positive Indian Ocean Dipole (IOD), when the western Indian Ocean warms but the sea offshore western Australia is colder than normal, is associated with droughts in SE Asia and Australia, especially in southeast Australia (Cai et al., 2009). Likewise, the El Niño state in the Pacific, when colder waters dominate in the western Pacific and the eastern Pacific is warmer than normal, weakens spring rains in Australia (Ashcroft et al., 2016). The IOD in particular has been affected by the closure of the ITF (Kajtar et al., 2015), although ENSO appears to be more dependent on the atmospheric Walker circulation (Sprintall et al., 2014). Nonetheless, restriction of the gateway is one of the factors driving long-term aridification of Australia (Krebs et al., 2011). Both ENSO and IOD are also affected by shorter-term orbital-related processes that affect the strength and seasonality of the rains and control the environment. El Niño conditions and thus weak Australian rains are more common when the Earth is generally warmer. Likewise, the IOD has become more positive, and thus Australia has been drier since the Last Glacial Maximum (LGM; 20 ka) (Abram et al., 2020).

Model-based testing of what controls monsoon intensity has been hampered by the lack of long-duration marine records. Although shallow piston coring has been effective in collecting sequences to examine how the monsoon has changed over millennial timescales, scientific ocean drilling is required to look at how this system has evolved on orbital (10^4) to tectonic ($> 10^6$ years) timescales. The work necessarily involves correlation of marine records with terrestrial sediment archives, as well as tectonic models derived from studying the mountains, whose uplift has influenced the atmospheric dynamics across the continents. Although continental records are important in providing some local control over environmental conditions and erosion of mountain belts, it is the marine depocenters that comprise the more continuous, better dated records that are required to develop sophisticated models of monsoon evolution and its impacts. The marine record is also critical if we are to relate the continental environmental conditions with the oceanography of the surrounding seas because understanding of the modern monsoon would indicate that they should be tightly coupled (Fasullo, 2012; Tada and Murray, 2016). Before the start of this most recent campaign of scientific drilling, there were major gaps in our data coverage, hampering better understanding. Although there were Miocene to Recent records from the Arabian and South China seas, no high-resolution records were available over many other parts of the region, at least spanning the Neogene, let alone the Paleogene. Since the onset of the monsoon has been estimated to be as old as the late Eocene (Licht et al., 2014; Sorrel et al., 2017), this made the marine record of rather limited use to study long-term evolution. Although it has long been argued that erosion and weathering of the mountains might be a primary control over global climate during the Cenozoic (Raymo and Ruddiman, 1992), the lack of a long-term erosional record from either of the large submarine fans in the Indian Ocean, let alone the major rivers of former Indochina prevented these models being tested.

2 Regional drilling campaigns

From 2013 to 2016, the International Ocean Discovery Program (IODP) conducted drilling around Asia and Australia that was specifically designed to document variations in monsoon intensity on millennial and longer tectonic timescales. This has resulted in significant revision of our reconstructions of when the monsoon intensified and weakened across a range of timescales, and in turn this contributes to our understanding of what the primary driving factors controlling wind and rainfall intensity in South and East Asia have been.

The drilling campaigns addressed all the marginal seas around Asia, stretching from the Arabian Sea in the southwest (Betzler et al., 2017; Pandey et al., 2016) to the Sea of Japan in the northeast (Tada et al., 2015), continuing southward through Indonesia, to the west coast of Australia (Gallagher et al., 2017) (Fig. 1). As well, both the major Indian Ocean submarine fans, the Indus and the Bengal (Clemens et al., 2016; France-Lanord et al., 2016), which together represent the bulk of the sediment derived from the Himalayan orogen, were drilled together with the Nicobar fan located on the east side of the Ninety-East Ridge and thus provide a relatively complete history of Himalayan erosion, at least covering much of the Neogene (McNeill et al., 2017). Furthermore, the eastern Indian Margin and Andaman Sea were drilled to reconstruct the Miocene to present monsoonal paleoclimate and paleoceanography (Clemens et al., 2016). In the South China Sea, three expeditions recovered sections of sediment mostly from the northern margin, related to the Pearl River catchment of southern China (Li et al., 2015; Sun et al., 2018), enhancing records obtained during the earlier ODP Leg 184 (Wang et al., 2000). Although drilling was largely focused on Neogene targets, for the first time the regional character of the campaign provided a wide sampling of many of the large continental drainage systems of Asia from which environmental, weathering, and erosion records can be derived, thus constraining both South and East Asian monsoons and providing the high-resolution records necessary for comparison between systems. Moreover, these are now accompanied by similarly high-resolution records from Western Australia looking at the evolution in climate of this continent and constraining the development of the monsoon system in that region, providing a means of comparison with the Asian monsoons (Gallagher et al., 2017). A related expe-
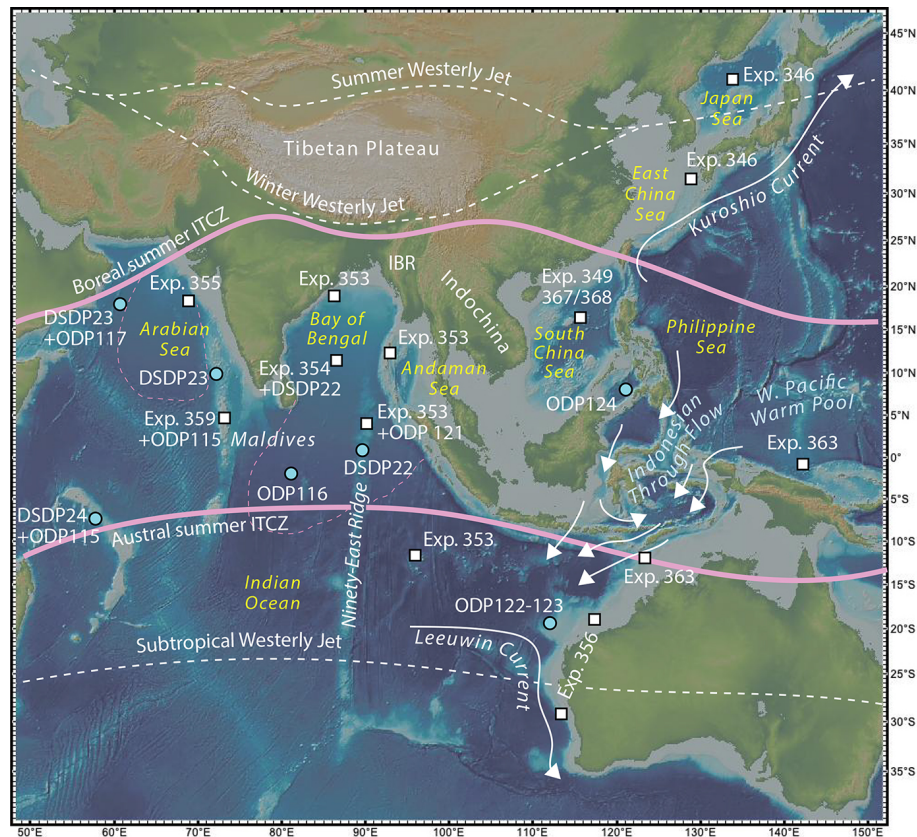
Figure 1. Shaded bathymetric map of the regions affected by the Asian and Australian monsoon systems showing the area of operations of the expeditions completed by IODP in the most recent campaign. Areas of older ODP and DSDP drilling are shown as blue dots. IBR is the Indo-Burman Range. Route of IFT after Gordon (2005). Dashed pink lines show outline of Indus and Bengal fans. ITCZ locations are from Yan (2005). Base map is from GeoMapApp.

dition offshore NW Australia and north of New Guinea provides an important record of the Western Pacific Warm Pool (WPWP) (Rosenthal et al., 2018), which is closely correlated with the intensity of the EAM system and additional Neogene records of the NW Australian system. In this study we summarize the primary findings in each of these critical areas and then assess how they may be related to one another in order to understand how different parts of the Asian–Australian monsoon system may be linked.

3 Arabian Sea

Some of the earliest constraints on the geological evolution of the monsoon were derived in the Arabian Sea through scientific drilling (Fig. 1). This is a particularly good area to look at the monsoon because of the strong oceanographic effects that the wind system has on upwelling and marine production in the area, as well as on the delivery of sediments from the Indian peninsula and particularly the Indus River, which represents the largest drainage system in the NW Himalaya. Prior to IODP drilling, the southwestern Indian margin was sampled by Indian National Gas Hydrate

Expedition 01 Site NGHP-01-01A, located offshore Goa. Sedimentary and geochemical data indicate stronger water mass mixing associated with a winter monsoon circulation after 23.7 Ma (Beasley et al., 2021). The same study also argued for the first summer monsoon after 23 Ma based on increases in Ti / Ca and dissolution of the biogenic carbonate fraction, as well as formation of an OMZ in the eastern Arabian Sea.

3.1 Expedition 355: environmental records in the Laxmi Basin

Expedition 355 recovered two long sections (1109 m penetration at Site U1456 and 1008 m at Site U1457) from the central Laxmi Basin, offshore western India, forming the eastern side of the Indus submarine fan. Recovery was 92 % with the advanced piston corer at Site U1456, 93 % at Site U1457 and 57 %, and 48 % with the Rotary Core Barrel (RCB) at each site respectively. The occurrence of a large mass transport complex (MTC) disrupted plans to recover sediment older than around 11 Ma (Dailey et al., 2019), but operations did retrieve a relatively continuous record of continen-

tal erosion spanning the last 11 Myr and covering the critical climatic transition around 8 Ma, albeit disrupted by a number of hiatuses (Routledge et al., 2020). Work within the NW Himalayan foreland had used carbon isotopes to identify changes in vegetation (Quade et al., 1989), and these same methods were applied to detrital organic carbon in the cores to assess how vegetation had evolved in the Indian peninsula and Himalayan foreland since 11 Ma. Studies of sedimentary organic carbon implied a change in the vegetation in the source regions starting at 7 Ma (Khim et al., 2020). The $\delta^{13}C$ of long-chain n-C_{32} fatty acids shifted from -34% to -22% between 10 and 6.3 Ma, and this was interpreted to indicate the progressive increase in C_4 grasses at the expense of C_3 plants (e.g., trees), especially between around 8.2 and 6.3 Ma (Suzuki et al., 2020) (Fig. 2d). This climatic transition was furthermore supported by a high-resolution study that focused on the period of climatic transition (Feakins et al., 2020). That study employed a multi-proxy approach involving bulk organic carbon and plant wax alkanes and acids, as well as a variety of pollen, charcoal, and lignin proxies, to assess how the vegetation changed under the influence of the evolving monsoon.

The Feakins et al. (2020) study was able to separate the influence of the Indus River compared to regional rivers draining the Indian peninsula. $\delta^{13}C$ values from n-C_{31} n-alkanes together with the other proxies supported the idea of expansion of grasslands through the late Miocene in northwest India, with change especially noted between 7.2 and 7.4 Ma. Interestingly, there was no clear change in δD values, which have been used as proxies for rainfall intensity in the Arabian Sea (Huang et al., 2007). This implied that there has been a relatively constant monsoon system across the area that was not disrupted during the time of transition in the vegetation and in turn raises the possibility that it was cooling, reconstructed from TEX_{86} data, and not drying that was responsible for the shift in the environment at that time.

Chemical weathering data has also been employed to constrain the evolving environment in the Indus catchment. Hematite / goethite values measured by color spectroscopy were used to constrain relative humidity, with hematite favored during times of drier climate. These records indicated a drying, or at least an increase in the duration of the dry season, after ~ 7.7 Ma, and while there was a phase of increased humidity between 6.3 and 5.9 Ma, a long-term trend was towards less chemical weathering and slower and drier conditions as the Miocene progressed into the Pliocene (Clift et al., 2020).

Bulk sediment major element geochemical data, color spectral data, and clay mineralogy confirmed a long-term decrease in weathering intensity that is often associated with drier, colder conditions (Zhou et al., 2021). The role of hematite in highlighting dry conditions is particularly noteworthy in implying a long-term decrease in humidity and thus summer monsoon rains (Fig. 2a). Clay minerals are sensitive to environmental conditions (Thiry, 2000) but can

also be used as provenance proxies under certain conditions. Clays have been used to argue that since 3.7 Ma, changes in monsoon strength have caused the sediment supplied to the Indian Ocean to alternate with more supply from the peninsula and Deccan Traps during times of heavier summer rains (Cai et al., 2020). It is noteworthy that there is a disconnect between monsoon intensity inferred from oceanic productivity records and those related to the climate. In the modern day, strong summer winds are associated both with heavy rain and with upwelling (Curry et al., 1992). This linkage extends to orbital timescales (Clemens et al., 2021) but does not appear to have been the case at longer timescales.

Nitrogen isotope compositions of sediment track marine nitrogen cycling, which can be related to biological productivity. N isotopes reflect the source of dissolved N to phytoplankton, and in nutrient-replete environments, the relative utilization. In the Arabian Sea, N isotopes reflect the upwelling of partially denitrified nitrate from the OMZ. Increases above the oceanic mean are taken as an increase in the intensity of the OMZ, often related to oxygen demand due to monsoon-driven upwelling (Altabet et al., 1995). N isotope and organic carbon contents of Laxmi Basin sediments indicate that the first sign of denitrification occurred at 3.2–2.8 Ma and that the modern OMZ was not established until ~ 1 Ma (Tripathi et al., 2017). Subsequent higher-resolution studies spanning 800 ka indicated a persistent OMZ in the eastern Arabian Sea but with a breakdown of the OMZ in the western Arabian Sea during glacial times when the summer monsoon weakened (Kim et al., 2018). Geological evidence for marine production and continental erosion implies that the summer monsoon strengthened at 2.95 Ma, possibly linked to closure of the ITF but then progressively weakened independently of the glacial climatic cycles (Sarathchandraprasad et al., 2021). The lack of correlation between the OMZ history and the terrestrial weathering and vegetation proxies is a clue that the paleoceanography and terrestrial rainfall are not tightly coupled over the longer-term geological past. This conclusion is consistent with a number of recent modeling studies (Nilsson-Kerr et al., 2021; Acosta and Huber, 2020).

3.2 Expedition 359: Maldives monsoon winds

The Maldives archipelago in the northern central Indian Ocean has acted for over 25 Myr as a giant natural sediment trap and contains a record of monsoon-related environmental changes in that region. The carbonate platforms record sea-level fluctuations, while the drift and periplatform deposits carry the record of monsoon-driven changes of the surface and intermediate water mass current regime and of wind-driven dust influx.

IODP Expedition 359 cored sediments from eight locations in the Inner Sea of the Maldives (Betzler et al., 2017). Penetration was up to 1097 m below the seafloor at Site U1467, located in the center of the Inner Sea, with
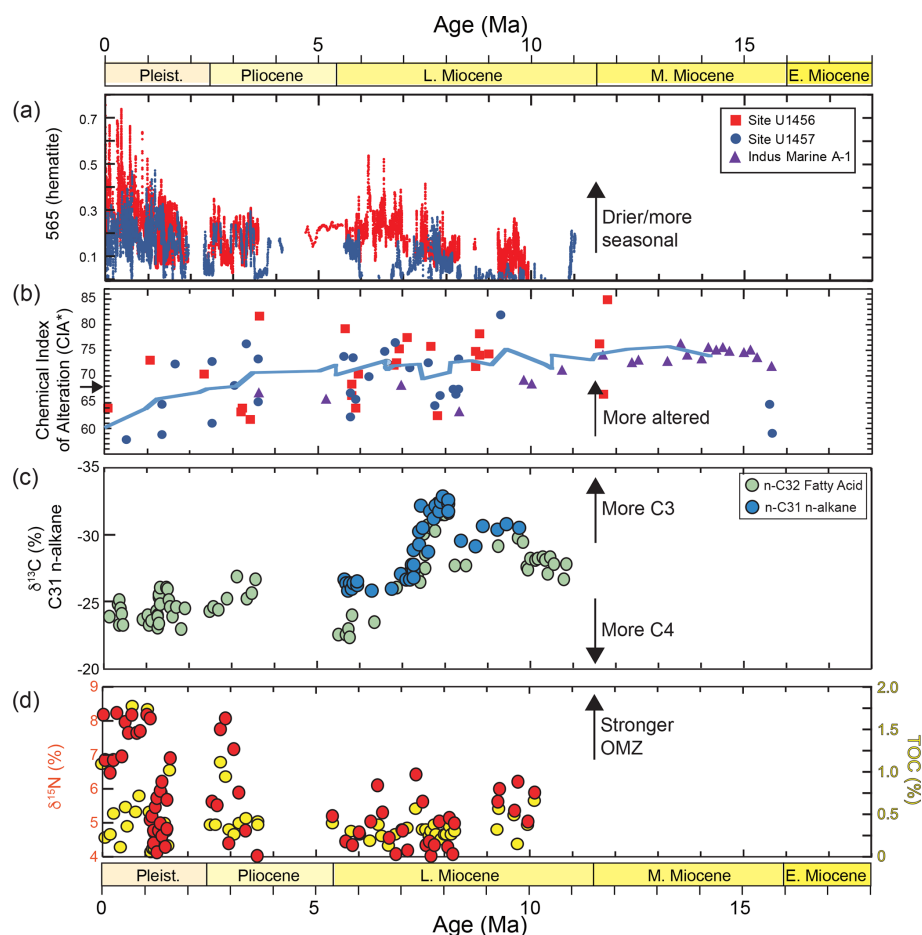
Figure 2. Temporal evolution in weathering proxies from the Laxmi Basin together with possible forcing factors. **(a)** 565 spectra intensity (hematite) and **(b)** CIA*, from Zhou et al. (2021), **(c)** $\delta^{13}C$ of n-C_{32} fatty acids (Suzuki et al., 2020) and from n-C_{31} n-alkanes (Feakins et al., 2020), and **(d)** $\delta^{15}N$ and total organic carbon (TOC) from Tripathi et al. (2017).

high degrees of recovery ($> 90\%$) over many of the intervals drilled by the APC. The expedition was designed to reconstruct the evolution of the South Asian monsoon (SAM) and related fluctuations of sea level. The timing of these changes is assessed by dating sedimentary alterations that mark stratigraphic turning points in the Neogene Maldives platform–basin system. The first turning points, dated as early and middle Miocene, are related mostly to sea-level changes. These are reliably recorded in the stratigraphy of the carbonate sequences in which sequence boundaries provide the ages of the sea-level lowstands (Vail et al., 1977).

An abrupt change in sedimentation patterns is recognized across the entire archipelago at a sequence boundary dated as 12.9–13.0 Ma (Betzler et al., 2016). At this turning point, the platform sedimentation switched to a current-controlled mode when the monsoon-wind driven circulation started in the Indian Ocean (Fig. 3). Several areas of the platform drowned in response to physical current effects, i.e., erosion and sediment re-deposition (Ling et al., 2021; Lüdmann et al., 2018; Reolid et al., 2020, 2019). The similar age of the

onset of drift deposition from monsoon-wind driven circulation across the entire archipelago indicates an abrupt onset of strong monsoon winds in the Indian Ocean (Betzler et al., 2016, 2018). Ten unconformities dissect the drift sequences, attesting to changes in current strength and/or direction that were likely caused by the combined impact of changes in monsoon wind intensity and sea-level fluctuations over the last 13 Myr. One major shift in the drift packages is dated with 5.8 Ma and coincided with a long-term sea-level rise that transformed the focused delta drift deposition to more widespread sheeted drifts (Fig. 3). A second major shift at 3.8 Ma coincided with the end of stepwise platform drowning and a reduction of the OMZ in the Inner Sea.

The strata of the Maldives platform provide a detailed record of the extrinsic controlling factors on carbonate platform growth through time. This potential of carbonate platforms for dating Neogene climate and current changes has been exploited in other platforms drilled by earlier scientific drilling. For example, Great Bahama Bank, the Queensland Plateau, and the platforms on the Marion Plateau show
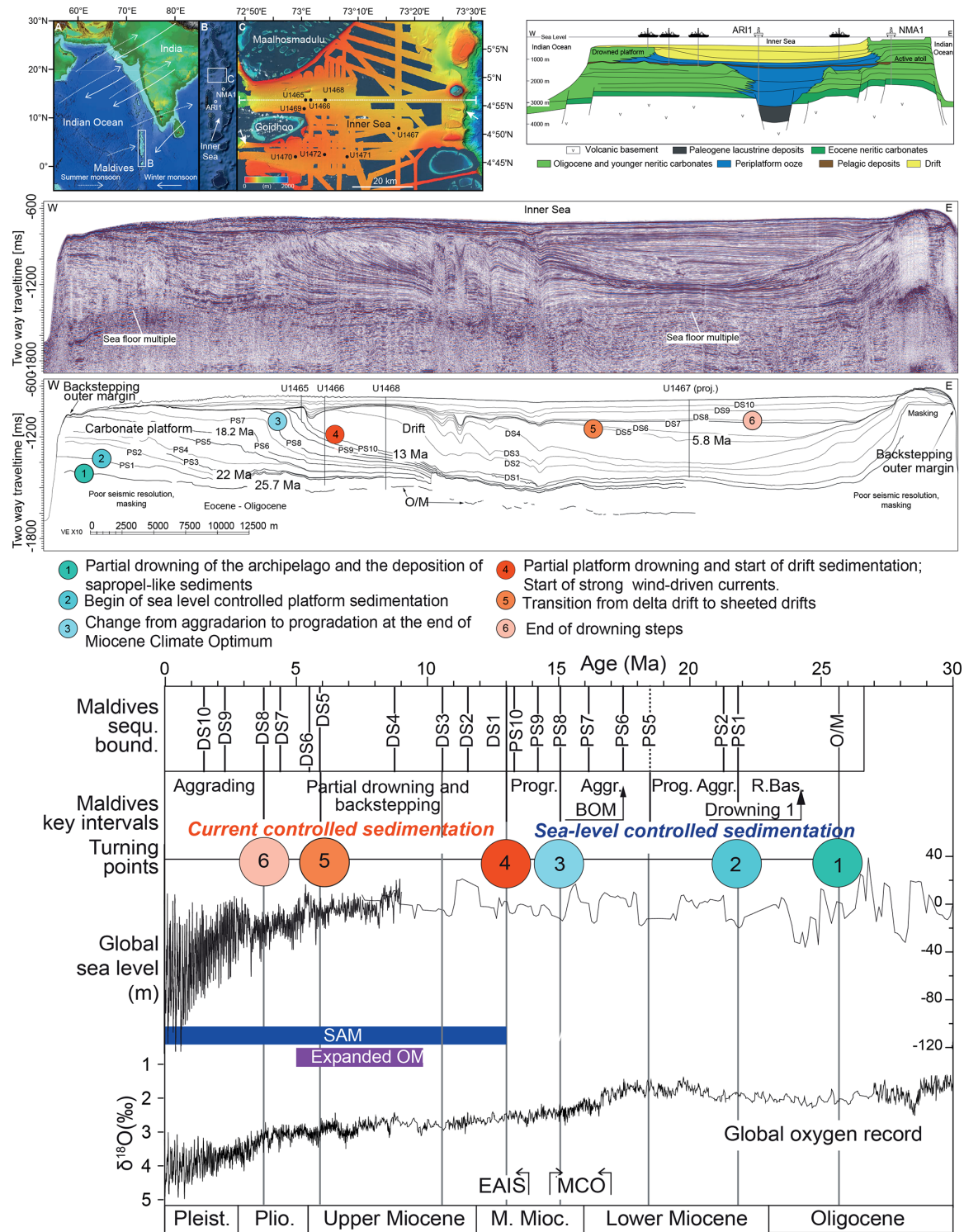
Figure 3. The Maldives archipelago, located in the Indian Ocean, is affected by the seasonally reversing monsoonal winds and currents. The archipelago has two rows of drowned and active atolls that line the Inner Sea. Seismic line across the Maldives Inner Sea with line drawing showing the platform sequence (PS) boundaries and the drift sequence (DS) boundaries. Carbonate platform sedimentation is controlled by sea level, while the drift sequences are controlled by strong currents which start at 13 Ma. Major turning points in sea level (blue circles) and current control (reddish circles) are indicated. Position of seismic line corresponds to white line in the map. Maps were produced using the program Esri ArcMap 10.1 (http://www.esri.com, last access: 29 May 2022). Bathymetric data were exported as Geotiffs from GeoMapApp 3.6.0 (http://www.geomapapp.org, last access: 29 May 2022). Worldwind satellite images (http://worldwind.arc.nasa.gov/java, last access: 29 May 2022) were merged with multibeam data acquired during cruises M74/4 and SO236.

similar histories with sediment architectures driven by sea level in their early history (early to middle Miocene) replaced by current-driven drowning or partial drowning during their later history (late Miocene) (Betzler and Eberli, 2019). In all three platform systems, the influence of currents on sedimentation is reported to be between 11 and 13 Ma.

The lithogenic fraction of the Maldives carbonate drifts provides a unique record of atmospheric dust transport during the past 4 Myr because grain size can act as a proxy for dust flux, as well as wind transport capacity (Lindhorst et al., 2019). Entrainment and long-range transport of dust in the medium to coarse silt size range is linked to the strength of the Arabian Shamal winds and the occurrence of convective storms that prolong dust transport. Dust flux and the size of dust particles increased between 4.0 and 3.3 Ma, corresponding to the closure of the ITF seaway and the intensification of the SAM. Between 1.6 Ma and the Recent, dust flux again increased but shows higher variability, especially during the last 500 kyr. Eolian transport capacity based on grain size increased between 1.2 and 0.5 Ma but has slightly decreased since that time. Dust transport varied on orbital timescales, with eccentricity control being the most prominent (400 kyr throughout the record and 100 kyr between 2.0 and 1.3 Ma and since 1.0 Ma). Higher-frequency cycles (obliquity and precession) are most pronounced in wind transport capacity.

Using XRF scans of the cores recovered at Site U1467, wavelet and spectral analyses of the Fe / K record show increased dominance of 100 kyr cycles after the Mid-Pleistocene Transition (MPT) at 1.25 Ma in tandem with the global ice volume inferred from calculated seawater $\delta^{18}O$ data (LR04 record) (Kunkelova et al., 2018). In contrast to the LR04 record, the Fe / K profile from Site U1467 resolves cycles that are similar to 100 kyr cycles around the 130 kyr eccentricity frequency band in the interval from 1.25 to 2.0 Ma. These cycles similar to 100 kyr cycles likely formed through the bundling of two or three obliquity cycles, indicating that low-latitude Indian–Asian climate variability reflected an increased tilt sensitivity to regional eccentricity insolation changes (pacing tilt cycles) prior to the MPT. The implication of appearance of the 100 kyr cycles in the LR04 and the Fe / K records since the MPT suggests strengthening of a climate link between the low and high latitudes during this period of climate transition.

4 Bay of Bengal

4.1 Expedition 353: South Asian monsoon

Expedition 353 (Clemens et al., 2016) drilled the Ninety-East Ridge, Bengal fan, northeast Indian Margin, and Andaman Sea. The expedition recovered 4.28 km of sediment from six sites with 97 % recovery on average. Double and triple coring was conducted in order to produce complete sections that would allow for reconstruction of continental erosion and monsoonal hydroclimate at a range of timescales from sites

with sedimentation rates ranging 2–15 cm kyr^{-1} (Robinson et al., 2016), with recovery spanning Campanian to Recent, although much of the Eocene was not recovered.

4.1.1 Paleocene–Oligocene: start of Himalayan erosion

Barnet et al. (2020) examined the interval of Earth history containing the well-known hyperthermal events of the Paleocene–Eocene Thermal Maximum (PETM) and Eocene Thermal Maximum (ETM), often studied as potential analogues for future anthropogenic climate change. Trace element and isotopic records from Ninety-East Ridge IODP Site U1443 and ODP Site 758 spanning $\sim$ 58–53 Ma place these hyperthermal events in the context of a long-term warming of the water column on the order of 4–5 °C. These results are comparable to those reconstructed from the low-latitude Pacific, demonstrating global-scale synchronous warming of the low-latitude and high-latitude regions of deep-water formation. These new findings support the idea that atmospheric CO_2 was the primary driver of global climate during this time of climatic transition.

Ali et al. (2021) used a newly-developed isotope chronostratigraphy from Site U1443 (Lübbers et al., 2019) coupled with samples from ODP Site 758 (at the same location) to evaluate the radiogenic Sr, Nd, and Pb isotopic composition of clay minerals produced from silicate weathering and deposited in the Bay of Bengal since 27 Ma, the longest such marine record in South Asia. They demonstrate remarkable source consistency, indicating dominance of supply from Himalayan rocks and the Indo-Burman Range, implying that the spatial pattern of weathering associated with monsoon rainfall has varied little over the past 27 Ma.

4.1.2 Miocene–Pliocene: changing Himalayan erosion patterns

A number of investigators have worked to differentiate provenance, weathering, tectonics, and climate change signals at Expedition 353 sites, located both in proximal and distal positions relative to the source drainages and using both hemipelagic and turbiditic sequences. Bretschneider et al. (2021) assessed high-resolution records of radiogenic Sr, Nd, and Pb isotopic composition of clay minerals deposited on the Ninety-East Ridge at Site U1443 across five time slices within the middle to late Miocene (15.8–9.5 Ma). This is the same site where Ali et al. (2021) recorded an increase in clay mineral abundance at $\sim$ 13.9 Ma that would signify an increase in physical weathering intensity in the sources, coincident with middle Miocene global cooling and regional tectonic reorganization (Fig. 4). Despite Himalayan tectonic reorganization, the erosional sources remained remarkably consistent across the five time slices. However, shorter (orbital) timescale variability shows significant fluctuations in all three isotope systems, likely linked to monsoon intensity. Variability within the middle Miocene Climatic Opti-
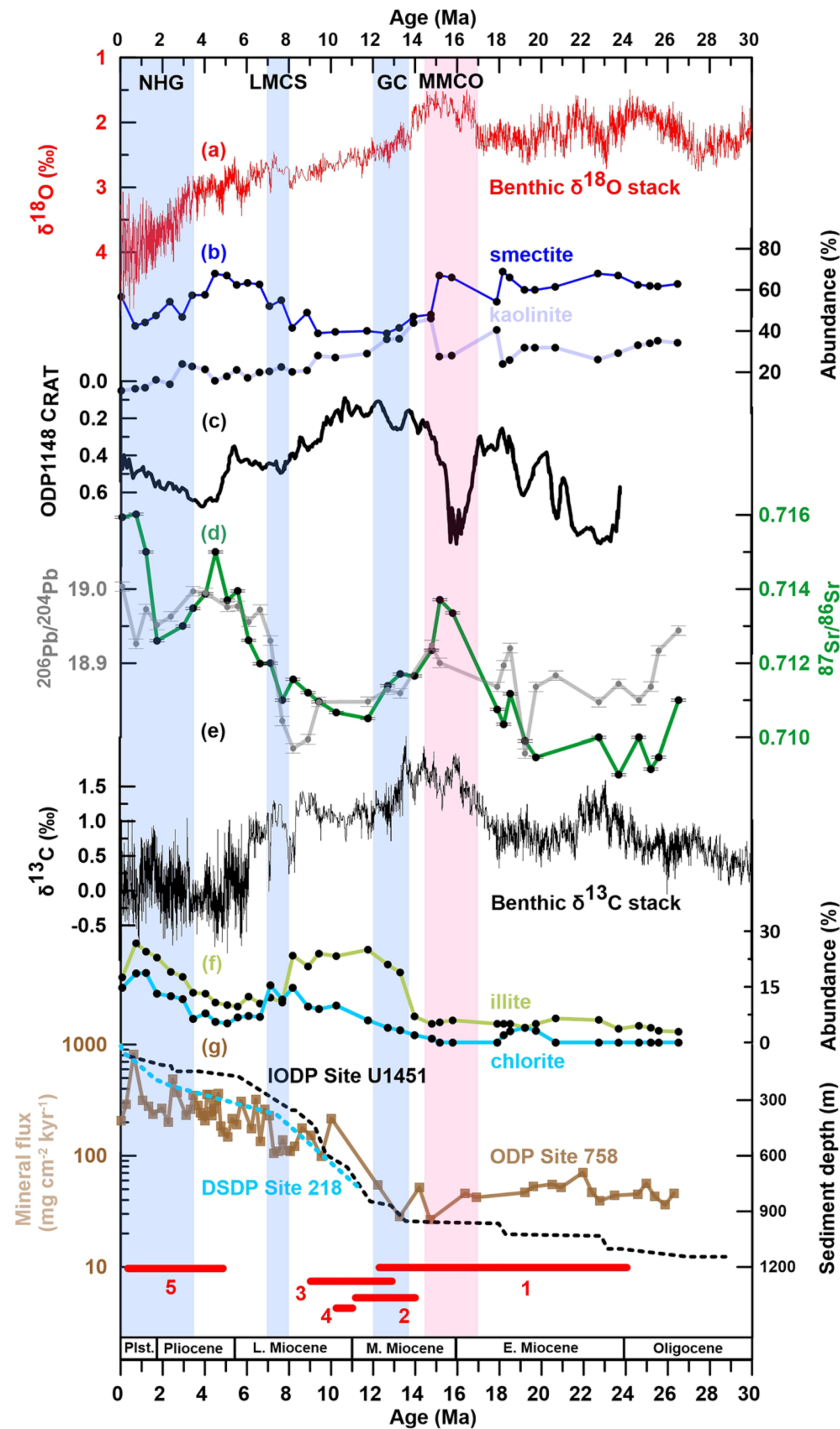
Figure 4. (a, e) Global $\delta^{18}O$ and $\delta^{13}C$ from bottom-living (benthic) foraminifera compiled from more than 40 DSDP and ODP sites (Zachos et al., 2008) representing global ice volume and deep-sea temperature, highlighting the global climate changes of the last 30 Myr. Periods of global cooling, after Zachos et al. (2008), are marked with blue bars, and the MMCO is marked with a red bar **(b, f)**. Clay mineralogy of ODP Site 758, relative abundances (% of smectite and kaolinite, illite, and chlorite), I CRAT record of ODP Site 1148 (Clift et al., 2008) from the South China Sea as a record of East Asian monsoon development, **(e)** Nd and Pb isotope composition of ODP Site 758 clays, **(g)** mineral flux record (Hovan and Rea, 1992) of ODP Site 758 recalculated using updated linear sedimentation rates, and sedimentation rates from the Bengal fan DSDP Site 218 and IODP Site U1451 (France-Lanord et al., 2016; Galy et al., 2010), and at the bottom a summary of the regional tectonic events (Allen and Armstrong, 2012). 1 – high Himalayan uplift, Main Central Thrust (MCT); 2 – onset of normal fault, southern Tibet; 3 – surface uplift, eastern Tibet; 4 – initial thrusting on main boundary Thrust; and 5 – fast exhumation at Himalayan syntaxes, outward growth of NE Tibet. This figure is from Ali et al. (2021).

mum (MMCO; 16–15 Ma) and the interval of global cooling at 13.9–13.8 Ma was larger than during younger intervals, a change attributed to movement of the precipitation locus from the high Himalaya to the frontal Himalayan ranges and to the Indo-Burman Range.

The older intervals from pelagic sections on the Ninety-East Ridge indicate relatively stable sediment provenance over long intervals of time. However, reconstructions from the middle–northern Bengal fan IODP Site U1444A, spanning the late Miocene to present (∼ 7–0 Ma), do indicate provenance changes. Chang and Zhou (2019) used optically and thermally stimulated luminescence (OSL and TL) of quartz and K-feldspar grains to characterize the sediment mineral composition through time. These authors interpret a distinct increase in quartz luminescence sensitivity at ∼ 3.5–0.5 Ma as increased hemipelagic contribution from Indian peninsular rivers relative to Himalayan-sourced pulses of turbidite sediments which dominated at 7–6 and 3.8–3.5 and since 0.5 Ma. In this case, changes between hemipelagic (Indian peninsula) and turbiditic (Himalayan) deposition were attributed more to changes in tectonic activity in the Himalayan region as opposed to the monsoonal climate.

Peketi et al. (2021) studied the time interval since ∼ 6 Ma at the eastern Indian continental margin Site U1445A using Sr and Nd isotopic analysis of the lithogenic fraction, elemental Fe / Al ratios, and clay mineralogy. They documented variable Ganga and Brahmaputra provenance at Site U1445A, with little input from the proximal Mahanadi drainage basin. The interval since 1.8 Ma indicates increased flux from the Brahmaputra River (supplied by erosion from the Trans-Himalayan batholiths) during periods of monsoon intensification and more from the Ganga during times of weakened monsoons. Variability within the interval 6–1.8 Ma was found to be influenced by both climate and tectonic forcings, the relative effects of which could not be differentiated.

Dunlea et al. (2020) also investigated the sequence recovered at Site U1445 to assess the expansion of C_4 vegetation, linked to drying of the environment. Their assessment of provenance was based on major, trace, and rare earth elemental concentration data, which were interpreted to indicate a Mahanadi drainage provenance, contrary to the conclusions of Peketi et al. (2021). The associated bulk organic and compound specific biomarkers, whether reflective of the Mahanadi drainage within the core monsoon zone of India or larger drainages to the north, document the existence of C_4 vegetation before the end of the Miocene but with an expansion to higher abundances at ∼ 3.5–1.5 Ma, all superimposed on an overall long-term decrease in monsoon precipitation since the late Miocene. These findings build upon the existing evidence for regionally heterogeneous responses in the timing of C_4 expansions and contractions, indicating sensitivity to regional climate changes in addition to global pCO_2 forcing (Feakins et al., 2020).

Hemipelagic sediment from western Andaman Sea Site U1447 spans the past 10 Myr and was analyzed by Lee et al. (2020b) for Sr and Nd isotopes, clay mineralogy, and δ^{13}C of sediment organic matter. The Nd and Sr data indicate sources in the Myanmar region, including major river drainages (e.g., Irrawaddy, Salween, Sittang) and smaller drainages from the Indo-Burman Range. Like the Ninety-East Ridge Site U1443 studies, the results indicate no significant changes in provenance since the late Miocene, and hence clay mineralogical changes can be interpreted in the context of monsoonal environmental change. A decreasing trend of smectite / (illite + chlorite) [S / (I + C)] implies stronger physical and weakened chemical weathering since the late Miocene, consistent with global cooling at that time. Climatologically, this is interpreted as a strengthening of the winter monsoon or weakening of the summer monsoon over this time period. Distinct events at 9.2–8.5, 3.6, 2.4, and 1.2 Ma were interpreted to result from the combined effects of global cooling and Tibetan Plateau uplift, the relative impacts of which cannot yet be differentiated. Initial results from spectral natural gamma ray (NGR) sediment core-logging and benthic foraminiferal stable isotope analyses of the upper Miocene record at Site U1447 indicate that an important long-term increase in physical weathering and erosion coincided with the globally recognized late Miocene cooling trend between ∼ 7.0 and 5.5 Ma (Kuhnt et al., 2020).

4.1.3 Miocene–Pliocene: monsoon-driven oceanic circulation

Lübbers et al. (2019) examined the critical interval of time from 13.5 to 8.2 Ma at Ninety-East Ridge Site U1443 using O and C stable isotopes from benthic foraminifera, XRF elemental data, and carbonate accumulation rates. At this equatorial site, a marked decrease in carbonate deposition took place between ∼ 13.2 and 8.7 Ma, coinciding with the middle to late Miocene "carbonate crash". Synthesizing the timing of this event at a global array of sites led the authors to hypothesize changes in chemical weathering and riverine influx of calcium and carbonate ions as fundamental mechanisms driving the carbonate crash and recovery. After 11.2 Ma, elemental ratio data (Ba / Ti) implied increased primary production and organic carbon burial. This timing, somewhat earlier than the global onset of the biogenic bloom, is attributed to intensification of upper-ocean mixing associated with changes in the seasonality and intensity of SAM winds and precipitation.

Jöhnck et al. (2020) produced a set of multi-proxy records from Site U1448 in the Andaman Sea spanning 6.24–4.91 Ma. Their benthic and planktic foraminiferal stable isotopes, combined with paired planktic carbonate Mg / Ca elemental ratio data, yield the first high-resolution orbital-scale reconstructions of monsoon variability across the Miocene–Pliocene transition. They found a 4 °C increase in mixed-layer temperature between 5.55 and 5.28 Ma, coincident with

a change from precession-dominated to obliquity-dominated variability in planktic $\delta^{18}O$ and seawater $\delta^{18}O$. This suggests that intensified cross-equatorial heat and moisture transport paced by obliquity resulted in increased summer monsoon precipitation during warm stages. In contrast, cold stages were characterized by colder mixed-layer temperatures and reduced monsoon rainfall, resembling Late Pleistocene stadials. The interval 5.55–4.91 Ma was one showing strong coherence of seawater $\delta^{18}O$ with orbital precession, indicating that seawater $\delta^{18}O$ minima lag precession minima by 119° (7.6 kyr). This lag is consistent with that measured in the Pleistocene from the same region (Gebregiorgis et al., 2018) and at Site U1446 on the northeast Indian margin (Clemens et al., 2021).

Most recently, a study of sediment from Ninety-East Ridge Site U1443 spanning the period 9 to 5 Ma reconstructed changes in biogenic production at high resolution and highlighted variance over cycles of 19–23 kyr, similar to that seen in the Late Pleistocene (Bolton et al., 2022). This work confirmed the important of insolation forcing of monsoon wind strength in the Indian Ocean and demonstrated that the wind system did not intensify significantly during the late Miocene.

4.1.4 Pleistocene: orbital forcing of monsoon productivity and rainfall

Monsoon variability has been assessed across the MPT, as well as orbital-scale variability over the past million years and high-resolution variability across marine isotopic stage 5 (MIS5). Lee et al. (2020a) evaluated paleo-productivity over the past 2.3 Myr at northeast Indian margin Site U1445 using the mass accumulation rate (MAR) of biogenic opal, total organic carbon (TOC), and total nitrogen to assess links between productivity and monsoon forcing across the MPT. These authors identified a regime change from a dominance of biogenic opal prior to the MPT to biogenic carbonate after this time. These changes were interpreted in the context of riverine silicate supply, with a strengthened monsoon-induced supply at 2.3–1.5 Ma, prior to the MPT, resulting in enhanced biogenic opal productivity. Across the MPT and thereafter, weakened monsoon runoff reduced stratification and enhanced nitrate supply from upwelling, leading to a carbonate-dominated productivity regime. The inferred reduction in monsoonal runoff is supported by the 0.19‰ shift in seawater $\delta^{18}O$ across the MPT observed at Site U1446 (Clemens et al., 2021).

Orbital-scale investigations of the monsoon at Andaman Sea Site NGHP-17/U1448 and northeast Indian margin Site U1446 have used water-related isotopes (speleothem $\delta^{18}O$, leaf wax δD, and seawater $\delta^{18}O$), leaf wax $\delta^{13}C$, and elemental XRF ratios to differentiate changes in the isotopic composition of rainfall from rainfall amount. McGrath et al. (2021) showed that variability in leaf wax δD is strongly coherent with that of speleothem $\delta^{18}O$, with variability in both proxies being coherent and in phase with ice-volume minima and pCO_2 maxima. In contrast, seawater $\delta^{18}O$ from the Andaman Sea (Gebregiorgis et al., 2018) and Indian margin (Clemens et al., 2021) indicates that maximum rainfall/runoff occurred significantly later and, in the case of precession, in phase with maximum summer-monsoon wind strength proxies. These relationships indicate that speleothem $\delta^{18}O$ and leaf wax δD predominantly reflect the isotopic composition of rainfall, varying as a function of changing moisture source areas and transport path dynamics, whereas seawater $\delta^{18}O$ predominantly reflects monsoonal rainfall and runoff amount.

Nilsson-Kerr et al. (2019) focused on millennial-scale seawater $\delta^{18}O$ and elemental ratio reconstructions of ice volumes during Termination II (TII; 139–127 ka) in the northeast Indian margin at Site U1446. They found that the TII is characterized by a transient monsoon intensification associated with the polar seesaw. The deglacial progression is characterized first by southern hemispheric warming, then by warming in the tropics, coincident with monsoon intensification, followed by northern hemispheric warming. These temporal relationships imply that the monsoon served as a conduit for the transport of heat across the Equator into the Northern Hemisphere, promoting deglaciation. This work was followed by a low-latitude synthesis of MIS 5 (130–70 ka) reconstructions combined with modeling (Nilsson-Kerr et al., 2021). Results document strong regional variability beyond that which can be ascribed to simple meridional migration of the ITCZ. Dipole-like patterns are pervasive across monsoon regions, highlighting the importance of mechanisms internal to the climate system, as opposed to monsoon systems responding simply external radiation forcing.

4.2 Expedition 354: Himalayan erosion and tectonics

Expedition 354 recovered long-duration erosion records going back to the Miocene in the central part of the submarine fan (Fig. 1). Coring followed a program of short APC cores, followed by extended core barrel (XCB) and finally RCB to the base of the section. The 17 holes drilled at Sites U1449–U1455 penetrated a total of 5167.2 m sub-seafloor. Coring spanned 2889.7 m of this penetration and recovered 1727.12 m of sediment and rocks (60 % average recovery). This expedition was designed to retrieve a complete record of turbidite deposition spanning the Neogene, together with more detail over the Pleistocene. The main objectives were to provide a record of erosion, both in terms of distribution and rate across the Himalayan arc, and a record of continental monsoon precipitation and vegetation and to estimate the impact of Himalayan erosion on the global carbon cycle. The E–W transect approach employed allowed the migration of the depocenter through time to be reconstructed and is the basis for reconstructing the paleo-erosion record (Fig. 5).
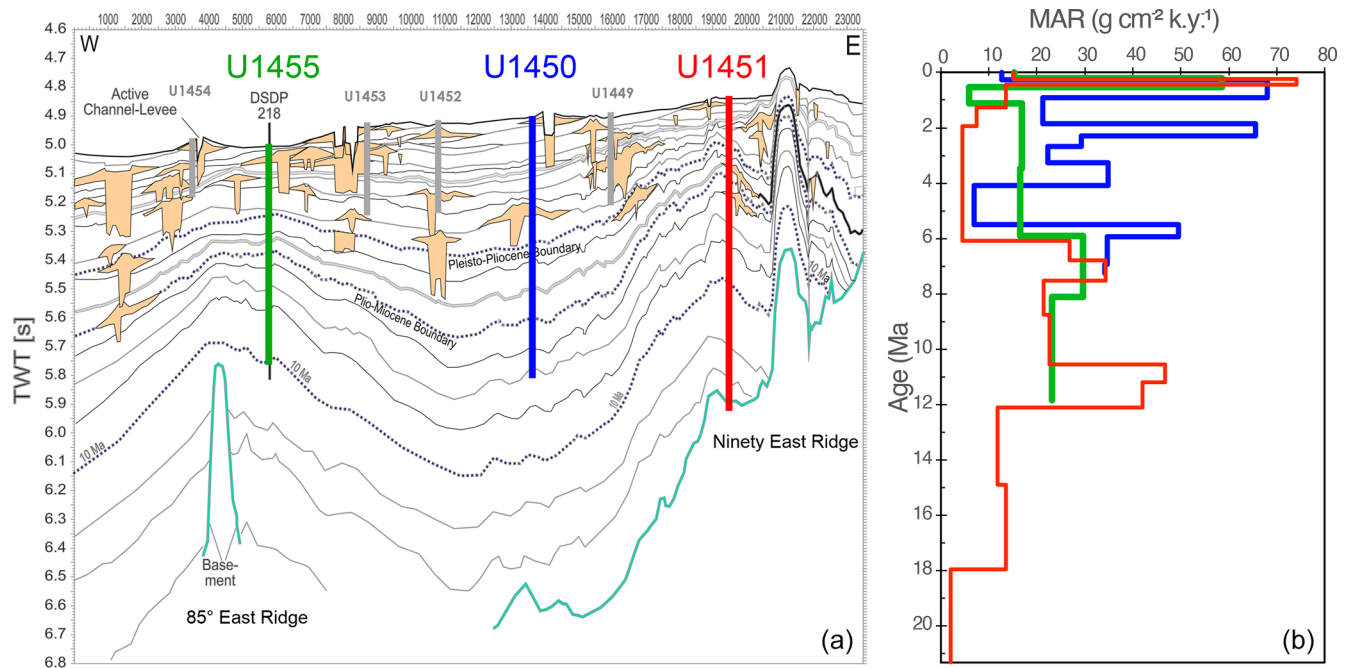
Figure 5. (a) Interpreted seismic section of the Bengal fan at 8° N (Schwenk and Spieß, 2009) with position of the Expedition 354 sites. The upper fan comprises a stacking of channel levee systems, with alternations of high accumulation of fan deposits and hemipelagic intervals that are 2 orders of magnitude lower. The easternmost Site U1451 drilled ∼ 1200 m on the west flank of the 90° E Ridge, where the onset of turbiditic deposition at this position has been dated around 18 Ma. Two other 900 m penetration sites (U1550 and U1455) complete the Neogene record. **(b)** Mass accumulation rates for the three deep records of Expedition 354. Age models are from France-Lanord et al. (2016), Lenard et al. (2020a), Cruz et al. (2021), and Reilly et al. (2020).

4.2.1 Turbidites of the Bengal fan

Sediments retrieved at all sites of Expedition 354 are dominated by turbidites composed of massive sand lobes and silty sand to clayey silt turbidites deposited by channel levee systems (Adhikari et al., 2018). Hemipelagic, calcareous clay layers mark intervals with no turbidite deposition. Sand deposition is estimated to represent up to 60 % of the sediments in the Pleistocene section (Bergmann et al., 2020) and was already widespread during the Miocene, reflecting strong erosion under a monsoon climate. In the absence of sand recovery in the deeper sections, high penetration rates and hole instability implied the presence of unconsolidated sand throughout the Miocene (France-Lanord et al., 2016). Petrologic and geochemical characteristics of turbidites are very similar to those of modern Ganga and Brahmaputra river sediments (France-Lanord et al., 2016; Yoshida et al., 2021). Their Sr–Nd isotopic compositions and heavy mineral geochronological characteristics further demonstrate the Himalayan lineage of these detrital sediments (Blum et al., 2018; Lenard et al., 2020b; Huyghe et al., 2020), making them suitable archives of how Himalayan erosion has responded to the changing climate.

4.2.2 Erosion of the Himalaya

The geochemical characteristics of the Bengal fan turbidites demonstrate their Himalayan origin. While this was known from earlier Deep Sea Drilling Project (DSDP) and ODP records (Galy et al., 2010) or Pleistocene cores (Hein et al., 2017; Joussain et al., 2017), for the first Expedition 354 allows for the time study of a complete Neogene to Holocene record, with minimum gaps in deposition and sediment transport bias. In addition, the abundance of sand layers and their efficient recovery by the half-length APC allowed for the sampling of up to 1 kg of sand and so access to dense mineral extractions for thermochronology or large samples of quartz grains for cosmogenic isotopes. Such methods are critical to reconstructing erosion and seeing how this related to monsoon intensity.

The distribution of U–Pb ages of detrital zircon reveals that in addition to the Himalaya, supply by erosion of the Asian plate, north of the Indus-Yarlung suture, was already as significant during the early Miocene, as it is today via the southern Tibetan connection of the Yarlung Tsangpo to the Brahmaputra (Blum et al., 2018). A multi-proxy reconstruction of provenance and exhumation rates employed apatite and rutile U–Pb, mica Ar–Ar, and zircon fission-track data. For sediments older than 10 Ma, the rutile and zircon fission-track thermochronometry shows lag times between cooling

and sedimentation that imply derivation from the Greater Himalaya, which were exhuming rapidly from 17 to 14 Ma, but then these slowed. Over the interval 5.6–3.5 Ma, lag times shortened to < 1 Myr, and only these are found since that time (Najman et al., 2019). This implies a speeding up of erosion since 5.6 Ma, especially from the eastern syntaxis centered on Namche Barwa. Najman et al. (2019) ascribe variations in erosion to tectonic forces in the Himalaya and syntaxis rather than the evolving monsoon climate, although we note that the SAM rainfall likely peaked around 15 Ma and then weakened in the late Miocene (Clift et al., 2008; Yang et al., 2020; Molnar and Rajagopalan, 2012).

Apatite fission-track lag times are more stable through time and translate in erosion rate to 1 to 3 mm yr^{-1} since the Miocene (Huyghe et al., 2020). Finally, for the first time on IODP cores, quartz in situ cosmogenic ^{10}Be concentrations were measured since 6 Ma (Lenard et al., 2020b). This study reported steady erosion rates of $\sim$ 1 mm yr^{-1} since the Miocene, implying that the onset of Pleistocene climate variability had little effect on the erosion regime.

4.2.3 Link to the carbon cycle

Himalayan erosion is potentially a globally significant actor in the carbon cycle. While silicate weathering is moderate in the drainage basin, the most important sink for carbon is thought to be via the burial of organic carbon (Galy et al., 2007). Detailed study of the weathering history is still in progress, but shipboard data on major element geochemistry and clay mineralogy already show that Bengal turbidites recovered at 8° N have relatively stable compositions and reflect essentially moderate intensity of silicate weathering. Overall K / Al ratios (a proxy for alteration intensity) of turbidites from Miocene to Holocene are similar to or higher than those of the modern rivers (Lupker et al., 2013), which indicates comparable to lower weathering conditions relative to today, consistent with results from the Arabian and South China seas (Clift and Jonell, 2021a). Similarly, clay mineral assemblages are dominated by illite and chlorite, which derives from physical erosion, not chemical weathering.

Shipboard organic carbon data confirm the general negative relationship between grain size and TOC in turbidites. Previous studies on Bengal fan turbidites demonstrated that they are dominated by organic matter exported from land and also carry indications of the evolution of vegetation. Shipboard data indicate that the organic carbon loading of the turbidites is slightly lower than observed in recent sediment in the northern part of the fan (Galy et al., 2008). However, a number of samples carry millimeter to centimeter organic particles that locally lead to very high organic carbon concentrations (Lee et al., 2019). These are derived from wood debris, whose δ^{13}C composition can be used to constrain the dominant vegetation. Miocene δ^{13}C values have a mean of −26.6‰, indicating C$_3$ dominance, but from about 4 Ma to present, the δ^{13}C of the wood is −20.5‰, which

is 3.3‰ more positive than the most ^{13}C-enriched sample during the Miocene. This suggests a mixture of C$_3$ and C$_4$ fragments. More ^{13}C-enriched values appear since 1 Ma, where δ^{13}C wood values are bimodal with a C$_4$-like cluster (mean = −13.1‰) as well as the typical C$_3$-like values (mean = −26.3‰). This suggests a change in the ecosystems from which the wood is being exported, with one-third of the wood derived from C$_4$ plants in the last 1 Myr. In addition to the permanent transfer of organic carbon with fine grained particles, low-frequency wood export contributed significantly to the carbon burial in Bengal turbidites.

On shorter timescales, Weber et al. (2018) investigated the role of orbital forcing in monsoon rainfall since 200 ka at Site U1452. The variability of TOC, total nitrogen, and the δ^{13}C composition of organic matter was used to indicate the marine origin of the organic matter, and this showed that primary marine productivity likely increased during times of enhanced NE monsoon during glacial periods. At the same time, there was faster delivery of sediment to the Bay of Bengal caused by higher soil erosion on land. Similarities between the sediment record and the Antarctic climate record spanning multiple glacial cycles imply a close relationship between high-southern-latitude and monsoonal Asian climate driven by shifts in position of the ITCZ.

5 South China Sea: chemical weathering and fluvial runoff

Since the first scientific oceanic drilling in 1999 (ODP Leg 184) in the South China Sea which focused on the theme of "Exploring the Asian monsoon", four more IODP expeditions (349, 367, 368, and 368X) have been completed since 2014. This later campaign was designed to examine the tectonic evolution of the South China Sea (Sun et al., 2018; Li et al., 2015). Nonetheless, these new expeditions recovered long sequences of sediment that can be used to study the Asian monsoon over geologic timescales.

During Expedition 349, a total of 703 and 611 m of sediment/sedimentary rock were recovered at the two deepest sites, Site U1431 in the central east subbasin and U1433 in the southwest subbasin (Li et al., 2015). Sedimentary magnetic parameters (magnetic susceptibility and ARM, anhysteretic remanent magnetization) and hematite / goethite values of sediment from Hole U1431D were used to infer EAM variation since 6.5 Ma (Gai et al., 2020). The magnetic results indicate that the EAM was stable between 6.5 and 5.0 Ma and intensified between 5.0 and 3.8 Ma, possibly due to closure of the Central American Seaway, and then weakened gradually starting after 3.8 Ma in response to the onset of Northern Hemisphere glaciation (NHG) and global cooling.

Pollen from IODP Site U1433, mainly derived from the Mekong River, shows a long-term increase in herbaceous plants since 8 Ma and indicates a persistent drying and weakening of precipitation in former Indochina (Miao et
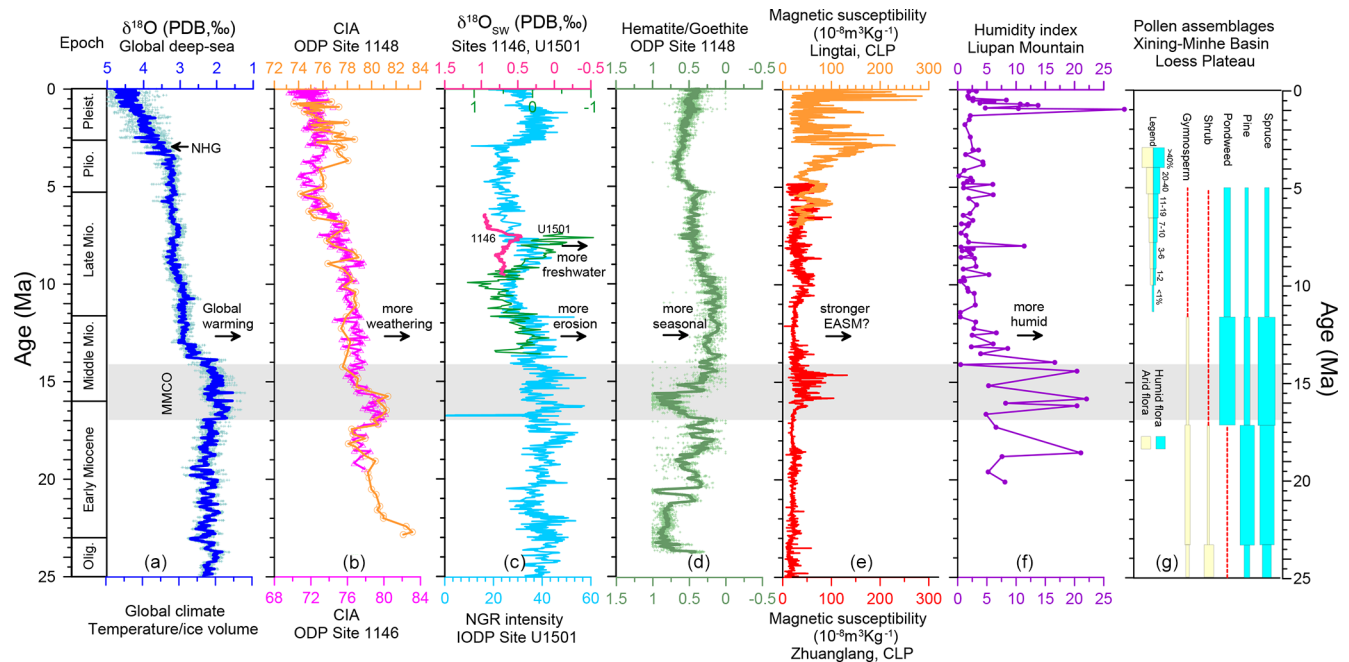
Figure 6. Proxies from land and sea showing the evolution of global climate and East Asian summer monsoon since 25 Ma. **(a)** Global deep-sea $\delta^{18}O$ (Westerhold et al., 2020); **(b)** chemical index of alteration at ODP Site 1146 (Wan et al., 2010) and 1148 (Wei et al., 2006) in the northern South China Sea; **(c)** seawater $\delta^{18}O$ at ODP Site 1146 (Steinke et al., 2010) and IODP Site U1501 (Yang et al., 2021), as well as NGR intensity at Site U1501 (Jian et al., 2018); **(d)** hematite / goethite ratio at ODP Site 1148 (Clift et al., 2008); **(e)** magnetic susceptibility of loess–paleosol sequences (Ding et al., 1999; Qiang et al., 2011); **(f)** pollen-based humidity index from Liupan Mountain (Jiang and Ding, 2008); **(g)** pollen assemblage evolution at Xining Basin (Sun and Wang, 2005). All drilling sites are located in the northern South China Sea on the continental margin.

al., 2017). Such an observation parallels trends in chemical weathering and hematite proxies at the same site (Liu et al., 2019). Interestingly, it remains debated as to whether the East Asian summer monsoon (EASM) intensified or weakened since the late Miocene (see synthesized proxies in Fig. 6). For example, magnetic susceptibility of loess–paleosol sequences suggests a weaker EASM during the Miocene–early Pliocene relative to late Pliocene–Pleistocene (An et al., 2001; Qiang et al., 2011; Zhao et al., 2020). In contrast, pollen assemblages in North China (Jiang and Ding, 2008; Sun and Wang, 2005) and weathering (Clift et al., 2014; Wan et al., 2010; Wei et al., 2006) and paleoceanographic proxies in the South China Sea (Holbourn et al., 2018; Steinke et al., 2010; Holbourn et al., 2021) show a general weakening EASM since the middle Miocene, possibly linked to global cooling.

Although IODP Expedition 368 recovered long sediment cores at Sites U1501 and U1505 on the continental margin in the NE South China Sea, most related studies are still on-going. However, at Site U1501 a study of seawater $\delta^{18}O$ and Mg / Ca ratios in planktic foraminifera has been completed. Differences between surface and thermocline records can be used to track the thermal gradient between the surface and subsurface waters, and the results imply that upper-water mixing was weaker at 9.4–7.3 Ma, which may have related to

increased fluvial runoff linked to higher rainfall. These data also suggest a decrease in the intensity of EASM between 13.6 and 10.2 Ma and an increase during 10.2–7.3 Ma (Yang et al., 2021). The trend in seawater $\delta^{18}O$ at Site U1501 is a little different from previous study at nearby ODP Site 1146 (Fig. 6), which shows a rapidly decreasing sea surface salinity (SSS) and weakening of EASM since 7.5 Ma (Steinke et al., 2010; Holbourn et al., 2018). In any case, a similar long-term decreasing trend in the intensity of NGR (indicative of terrigenous clay input) is observed at both sites (Jian et al., 2018), consistent with a coupled evolution of continental erosion and monsoonal rainfall. This record implies that late Miocene rainfall of South China might have become wetter, while that in South Asia was drying after 7 Ma, a discrepancy that Yang et al. (2021) linked to formation of the WPWP at this time influencing East Asia, while Indian Ocean surface water cooling and Tibetan uplift were more influential in South Asia.

6 Sea of Japan: paleoceanography and Asian dust records

Expedition 346 targeted the upper Miocene to Holocene hemipelagic sediments of the Sea of Japan (East Sea of Korea) and the northern East China Sea (ECS) (Fig. 7). Seven

sites were drilled in the Sea of Japan, with two closely spaced sites in the ECS. In total, the expedition recovered 6135.3 m of core by the APC, with an average recovery of 101 %.

The primary objective was to explore the timing of onset and evolution of millennial- and orbital-scale variabilities of the EAM based on the hypothesis of Tada et al. (1999, 2015) that millennial- and orbital-scale variabilities of the EAM were recorded in the hemipelagic sediments of the Sea of Japan. These deposits are characterized by centimeter- to decimeter-scale alternations of dark and light layers modulated by the fresh-water discharge of the Yangtze River during summer that diluted the surface water of the northern ECS and modulated the SSS and nutrient concentration of the ocean water flowing into the Sea of Japan through the Tsushima Strait. Changes in SSS and nutrient content of the ocean water flowing into the Sea of Japan caused changes in ventilation and surface productivity of the sea.

Clemens et al. (2018) analyzed δ^{18}O and Mg / Ca ratios of *G. ruber* at Site U1429 in the northern ECS and reconstructed δ^{18}O$_{sw}$, which reflects runoff-induced changes in SSS, during the last 400 kyr. They demonstrated that local SSS changed in association with eccentricity and obliquity cycles but not with the precession cycle, although precession is clearly evident in the planktonic δ^{18}O. This contrasts the work of Cheng et al. (2016), who demonstrated that δ^{18}O of Chinese stalagmites shows a strong precession signal, with almost no evidence of eccentricity and obliquity. Hence, the extent to which local precipitation is reflected in stalagmite δ^{18}O remains in question. Clemens et al. (2018) also demonstrated the presence of millennial-scale variability of δ^{18}O$_{sw}$, which Kubota et al. (2019) interpreted to reflect changes in precipitation of EASM in association with Dansgaard–Oeschger cycles during the last glacial period. Kubota et al. (2019) also demonstrated that δ^{18}O$_{sw}$ changes in the northern ECS are closely associated with the changes in the gray scale of the sediments in the deeper part of the Sea of Japan, consistent with the hypothesis of Tada et al. (1999, 2015).

Irino et al. (2018) revised shipboard splices and constructed a complete, continuous dark–light sedimentary sequence at the seven sites drilled in the Sea of Japan, covering the last 3 Myr. Tada et al. (2018) used this sequence to examine centimeter- to decimeter-scale dark layers for the six sites deeper than ∼ 900 m water depth. They confirmed that it is possible to correlate almost all of the dark layers between the six sites in the deeper part of the basin, which could be traced back to 1.45 Ma when the first distinct dark layer was deposited. It was concluded that the Sea of Japan has responded to the orbital- and millennial-scale climatic changes as a single system since 1.45 Ma and that intermittent occurrences of millennial-scale variability of EAM can be traced back to at least 1.45 Ma. Based on XRF core scanning, Seki et al. (2019) demonstrated that gray-scale variation of Sea of Japan sediments basically reflects marine organic carbon content and so in turn reflects millennial-scale variability of the surface productivity.

Tada et al. (2018) also demonstrated that gamma ray attenuation density (GRA) is controlled by diatom content and that this changes in association with glacio-eustatic sea-level changes. Using this relationship, they constructed an orbitally tuned age model covering the last 3 Myr. Kurokawa et al. (2019) extended this age model back to 11.7 Ma, allowing for precise dating of paleoceanographic events across the basin. For example, they identified the occurrence of a hiatus from 7.3 to 5.3 Ma at Site U1330 on the South Korean Plateau, at water depths of 1072 m. It is possible that this hiatus was caused by intensification of the Sea of Japan Intermediate Water during the late Miocene global cooling (LMGC) interval from 7.8 to 5.8 Ma (Herbert et al., 2016).

Matsuzaki et al. (2020) examined radiolarian assemblages at Site U1425 in the middle of the Sea of Japan spanning the time interval 9.1–5.3 Ma and used these to reconstruct annual mean sea surface temperature (SST). They found a drastic decrease in annual SST from 24 to 16 °C from 7.9 to 6.6 Ma, which they attributed to intensification of East Asian winter monsoon (EAWM) during the early half of the LMGC. Based on comparison with NW Pacific high-latitude and midlatitude alkenone-based SST (Herbert et al., 2016; LaRiviere et al., 2012), they speculated that the later half of LMGC is characterized by summer cooling.

Shen et al. (2018) analyzed δ^{13}C of black carbon of probable eolian origin in sediments from Site U1430 and found a drastic increase in δ^{13}C that started at ∼ 5.3 Ma. They argued that this increase most likely reflects expansion of C$_4$ vegetation in Central Asia. However, they used a preliminary age model which did not take into account the hiatus from 7.3 to 5.3 Ma. According to a new age model of Kurokawa et al. (2019), the drastic increase in δ^{13}C occurred during the hiatus between 7.3 and 5.3 Ma. It is likely that expansion of C$_4$ vegetation in Central to East Asia occurred in association with LMGC.

Anderson et al. (2020) reconstructed the provenance of aluminosilicate sediment at Site U1430 since 12 Ma using multivariate partitioning of the major, trace, and rare earth element composition of bulk samples. They identified four aluminosilicate components (Taklimakan, Gobi, Chinese Loess, and Korean Peninsula) and demonstrated that the Taklimakan Desert component was the most abundant component before 7.5 Ma, whereas Gobi + Chinese Loess components became dominant by 4 Ma (and maybe as early as 7.5 Ma when taking into account the hiatus between 7.3 and 5.3 Ma) (Fig. 8). Accumulation rates of these dust components were relatively high before 7.5 Ma and very low between 4 and 2 Ma and increased again after ∼ 2 Ma. It is possible that expansion of the Gobi Desert and Chinese Loess Plateau occurred in association with LMGC. Because sedimentation at Site U1430 was influenced by bottom current winnowing from 7.5 Ma to as young as 3.5 Ma, similar provenance studies should be
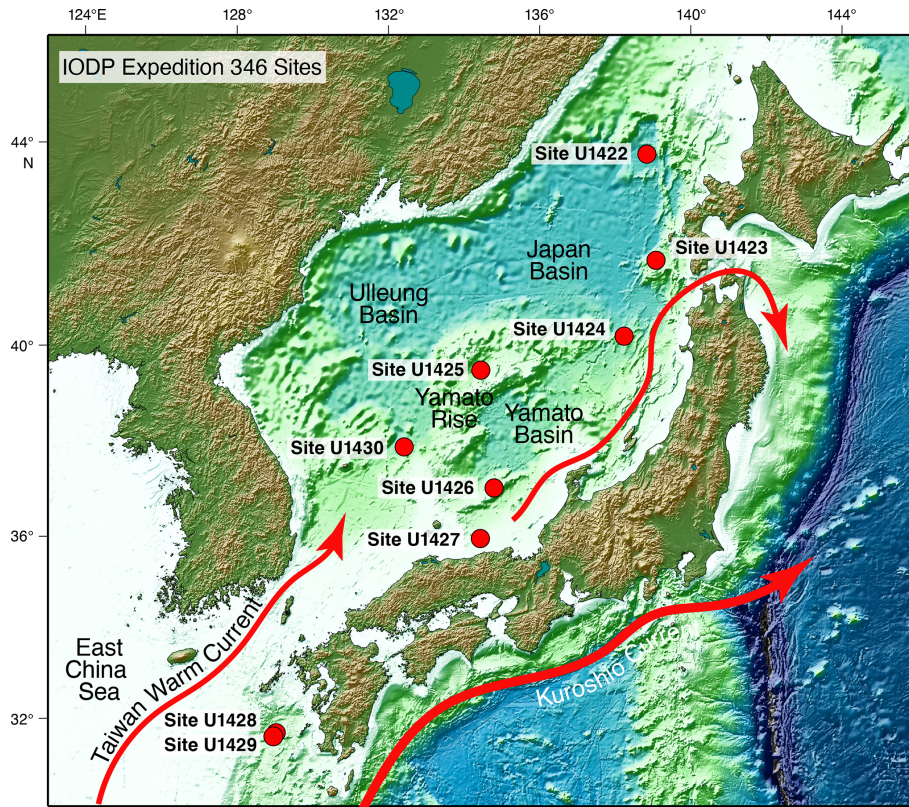
Figure 7. Bathymetric map of the area sampled by Expedition 346 with the major bathymetric features labeled as well as the locations of the drilling site. The red arrows show the major surface currents that affect the region. Modified after Tada et al. (2015).

conducted at other deeper-water sites to evaluate dust flux during the time interval between 7.5 and 1.5 Ma.

Results of Expedition 346 proved that dark and light alternations of the Quaternary sediments from the Sea of Japan faithfully recorded millennial-scale variability of EASM. Changes in salinity and nutrient concentration of the influx through the Tsushima Strait into the Sea of Japan since 1.45 Ma controlled surface productivity and ventilation in the sea so that millennial-scale variability of EAM can be traced back to that time. The work showed that distinct precession signals recorded in $\delta^{18}O$ of Chinese stalagmites were not caused by local precipitation changes of EASM but more likely reflecting changes in the $\delta^{18}O$ of precipitation, whereas millennial changes in $\delta^{18}O$ of Chinese stalagmites probably reflect changes in EASM precipitation. It is highly likely that EAWM intensified during the early half of the LMGC. On the other hand, EASM seems to have been weakened later during LMGC. It is possible that Gobi Desert expanded and C_3 to C_4 transition of vegetation occurred in Central to East Asia in association with the LMGC. However, the presence of a hiatus from 7.3 to 5.3 Ma in the sedimentary record of Site U1430 precludes precise dating of their timings. Similar examinations at Site 1425 are desirable.

7 Western Australian monsoon

North Australia is influenced by strong summer westerly and southwesterly winds that source warm, moist equatorial air, leading to monsoonal rains and cyclonic activity north of the monsoon shear line (Fig. 9). Seasonal monsoonal runoff delivers substantial amounts of fluvial sediment to the shelf via the Fitzroy, De Grey, Ashburton and Fortescue rivers. In contrast, continental wind-blown dust is transported by the trade winds offshore northwest Australia when the trade winds dominate during the winter dry season (Fig. 9).

IODP Expedition 356 cored seven sites to determine the latitudinal variation in climate and ocean conditions from ~ 30 to 18° S over the last 5 myr (Gallagher et al., 2017). The expedition recovered 5185.15 m of core, with 62 % recovery. Sites were cored in shelf regions near to the shore to determine the long-term history of the Australian monsoon and southwestern Australian climate. Many sites yielded older sections, revealing a climate archive extending as far back as ~ 50 Ma. For example, Sites U1461 and U1462 on the NW continental shelf at $\sim 22^\circ$ S yielded thick (up to 1 km) sections of upper Miocene to Recent strata that record the southerly extent of the Australian monsoon and its intensity. Further north, Sites U1463 and U1464 ($\sim 18^\circ$ S) cored middle Miocene to Recent sections with contrasting facies
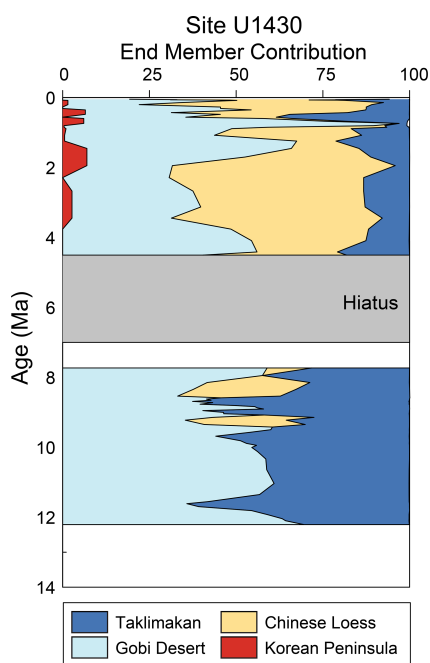
Figure 8. Aluminosilicate contribution (wt % of aluminosilicate inventory) at Site U1430 through time. The end-member contributions are plotted as the total sum, with each color representing the sum of the specific end-member plus the end-members to the left. The shaded region denotes a hiatus, and the following box notes a period in which we did not overinterpret our data to fill the temporal gap between the end of the hiatus and the start of our Miocene-aged samples. From Anderson et al. (2020).

ranging from Miocene subaerial, arid, sabkha evaporitic facies (Groeneveld et al., 2017; Tagliaro et al., 2018), and Pliocene deep-water carbonates (De Vleeschouwer et al., 2018) to Quaternary aridity-related oolite facies (Gallagher et al., 2018). These cores provide an unprecedented opportunity to investigate the long-term history of the Australian monsoon and aridity.

Previous studies suggested that at 23–14 Ma, Australia experienced seasonally wetter, monsoonal rainfall compared to today when the monsoonal front was in a similar position (Herold et al., 2011). However, analyses of sediments from Site U1459 show that arid conditions persisted from 16 to 6 Ma (Groeneveld et al., 2017), transitioning to a wetter period with all-year-round rainfall at ∼ 5.5 Ma (Site U1463) (Christensen et al., 2017; De Vleeschouwer et al., 2018; Auer et al., 2019) that became seasonal (monsoonal) starting at ∼ 3.3 Ma. The drying trend exhibited in Miocene NW Australia is broadly similar to that seen in the Mekong basin, and there may be a relationship between the northward migration of the westerlies from ∼ 12 Ma associated with expanded Antarctic sea ice and its abrupt shift back associated with LMGC (Groeneveld et al., 2017). The onset of humidity in NW Australia occurred seemingly differentially, first at the more northerly Site U1464 ∼ 6 Ma (Groeneveld et al.,

2017) and later at Site U1463 at ∼ 5.5 Ma (Christensen et al., 2017). However, Karatsolis et al. (2020) suggested the region was humid, probably since ∼ 7 Ma when the ITCZ moved southward. NW Australia remained in the Humid Interval until ∼ 3.3 Ma (Christensen et al., 2017) when conditions became drier, although a major SST drop from ∼ 3.15 to 3 Ma based on TEX_{86} indicates temperature-driven drying may have begun slightly later (Smith et al., 2020). NW Australia achieved arid conditions with a strong winter monsoon similar to today by ∼ 2.4 Ma at the onset of the Arid Interval (Christensen et al., 2017) when higher-amplitude interglacial–glacial fluctuations in SST (Smith et al., 2020) led to a seasonal (monsoonal) regime. Over the last 2 Myr, interglacial wetter (strong monsoon with clay influx) and arid glacial (weak monsoon with limestone facies and dust input) conditions persisted in Australia's northwest (Gallagher and deMenocal, 2019). Evidence of the Holocene Australian summer monsoon (ASM) activity has been interpreted at Site U1461 from K / Ca ratios, with the percentage of potassium constrained from shipboard NGR (Ishiwa et al., 2019). These data show increased fluvial terrigenous input after 11.5 ka, followed by a maximum at ∼ 8.5 ka due to enhanced ASM-derived precipitation as a response to the southern migration of the ITCZ. Subsequently, weakening of rainfall after 8.5 ka was caused by the northern migration of the ITCZ.

8 Western Pacific Warm Pool

As a major source of heat and moisture to the atmosphere, the WPWP, often defined by the 28 °C isotherm and located in the heart of the Indo-Pacific Warm Pool, exerts a major role in influencing climate both in the tropics and globally. Changes in the SST of the WPWP influence the location and strength of convection in the rising limb of the Hadley and Walker cells, affecting planetary-scale atmospheric circulation, atmospheric heating, and tropical hydrology, including the Asian and Australian monsoons (Neale and Slingo, 2003; Wang and Mehta, 2008). Likewise, an important control on the WPWP and east Asian hydroclimate is the change in the equatorial Pacific zonal and Equator to pole temperature gradients. A primary goal of Expedition 363 was to assess changes in regional climate variability, expressed in temperature, precipitation, and biological productivity in the context of the global background state from the middle Miocene through the Holocene.

Currently, there is an ongoing debate about the evolution of SST in the WPWP since the late Miocene, due to substantial disagreement between proxy records, whereas foraminiferal Mg / Ca suggests stable mixed-layer temperatures throughout this period; records of the organic proxy TEX_{86}, interpreted to reflect SST, argue for a major cooling throughout with a similar magnitude to the change observed in the eastern equatorial Pacific (Zhang et al., 2014b; Ravelo et al., 2014; Zhang et al., 2014a). These two con-
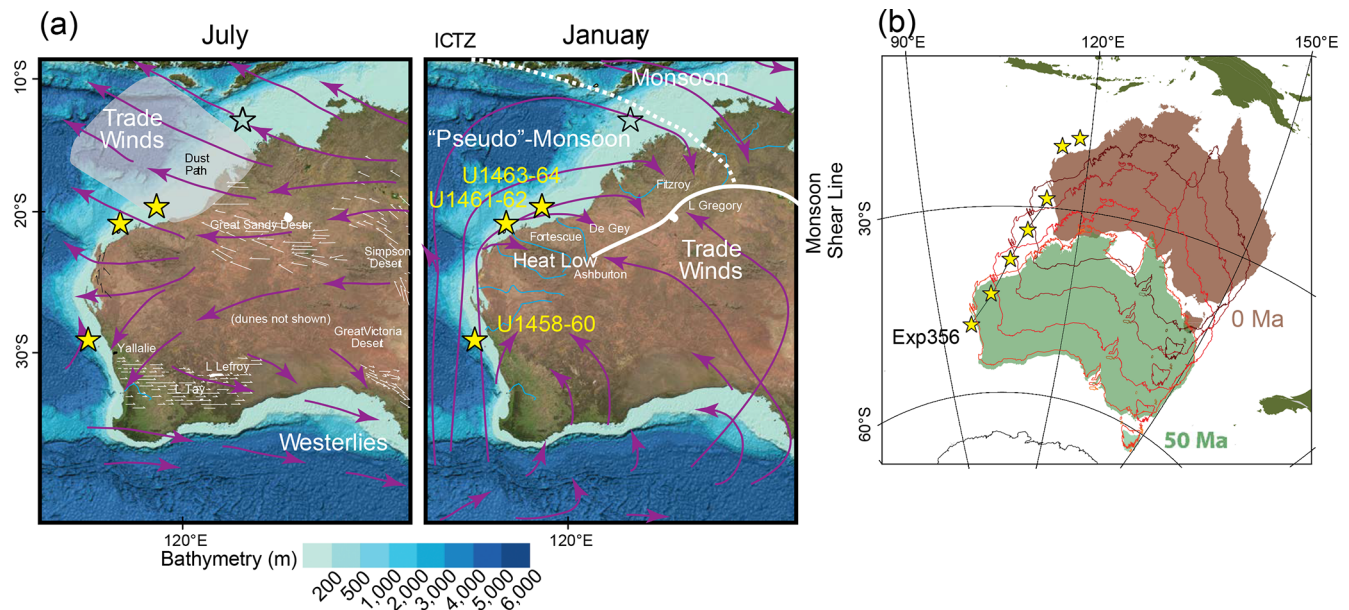
Figure 9. (a) Atmospheric circulation for January and July (Gentilli, 1972) with the mean monsoon shear line (McBride, 1986) and intertropical convergence zone (ITCZ). Base map adapted from the General Bathymetric Chart of the Oceans (GEBCO) http://www.gebco.net (last access: 29 May 2022). IODP Expedition 356 sites are shown as stars. **(b)** Plate tectonic motion of Australia since 50 Ma at 10 Myr intervals, with the path line for Site U1459 (Expedition 356). Figure adapted from Gallagher and deMenocal (2019).

trasting scenarios of the evolution of the equatorial Pacific zonal temperature gradient have very different implications on the hydroclimate of the Indo-Pacific Warm Pool and likely the Asian monsoon system. However, using samples from IODP Site U1488, Meinicke et al. (2021) show very good agreement between measurements of mixed-layer and thermocline planktic foraminiferal Mg / Ca and clumped isotopes (Δ_{47}), two independent foraminiferal proxies of temperature, thereby supporting the view that the WPWP mixed-layer temperatures did not cool substantially since the early Pliocene, while subsurface temperatures cooled more strongly, a change analogous to a shift from El Niño-like to more La Niña-like conditions, which could have intensified regional precipitation in the WPWP and east Asia.

Seasonal to interannual climate variations in the WPWP are dominated by fluctuations in precipitation associated with the seasonal march of the monsoons, migration of the intertropical convergence zone (ITCZ), and interannual changes associated with variability of the El Niño–Southern Oscillation (ENSO). It has been argued that on orbital timescales, the ITCZ and associated tropical precipitation belt migrate from a northern- to southern-centered position, relative to the Equator. These hemispherically asymmetric shifts are in pace with orbital variability. In contrast, new XRF geochemical records from Site U1483 and nearby sites on the northwestern Australia margin, when compared with published precipitation records from the WPWP, suggest that precipitation changed nearly in phase between the two hemispheres on the precession band, arguing for expansion and

contraction in the latitudinal extent rather than migration of the tropical precipitation belt (Zhang et al., 2020). Furthermore, XRF records from other sites further to the south on the Australian, including Site U1482, reveal shorter periods of maximum Australian monsoon in the early Holocene (~ 10 ka), MIS 5e (~ 130 ka), MIS 7 (~ 200, ~ 220, and ~ 240 ka), and MIS 9 (~ 280, ~ 305, and ~ 330 ka), when maxima in atmospheric greenhouse gases coincided with maxima in Southern Hemisphere insolation (September). The intensification of the regional monsoon is attributed to intensely heated low-pressure cells over the Pilbara region that trigger the southward shift of the ITCZ (Pei et al., 2021). When compared with sites recovered in the other expedition, it is clear that the ongoing research on sites recovered during Expedition 363 will be important in testing hypotheses related to regionality and globality of the monsoon system, both on orbital and shorter timescales.

9 Synthesis

Comparison of the monsoon records in the different drilling areas targeted in this campaign indicates drying trends in most parts of Asia since ~ 10 Ma, which contrasts with the NW Australian wet phase at 5.0–2.5 Ma. However, this area too shows a trend to drier environments after 2.5 Ma (Fig. 10). Decoupling of the Australian and Asian monsoons reflects the greater influence of the ITF over regional climate in the Southern Hemisphere. Even within Asia, drying of the continent has not occurred in a uniform fashion. While most
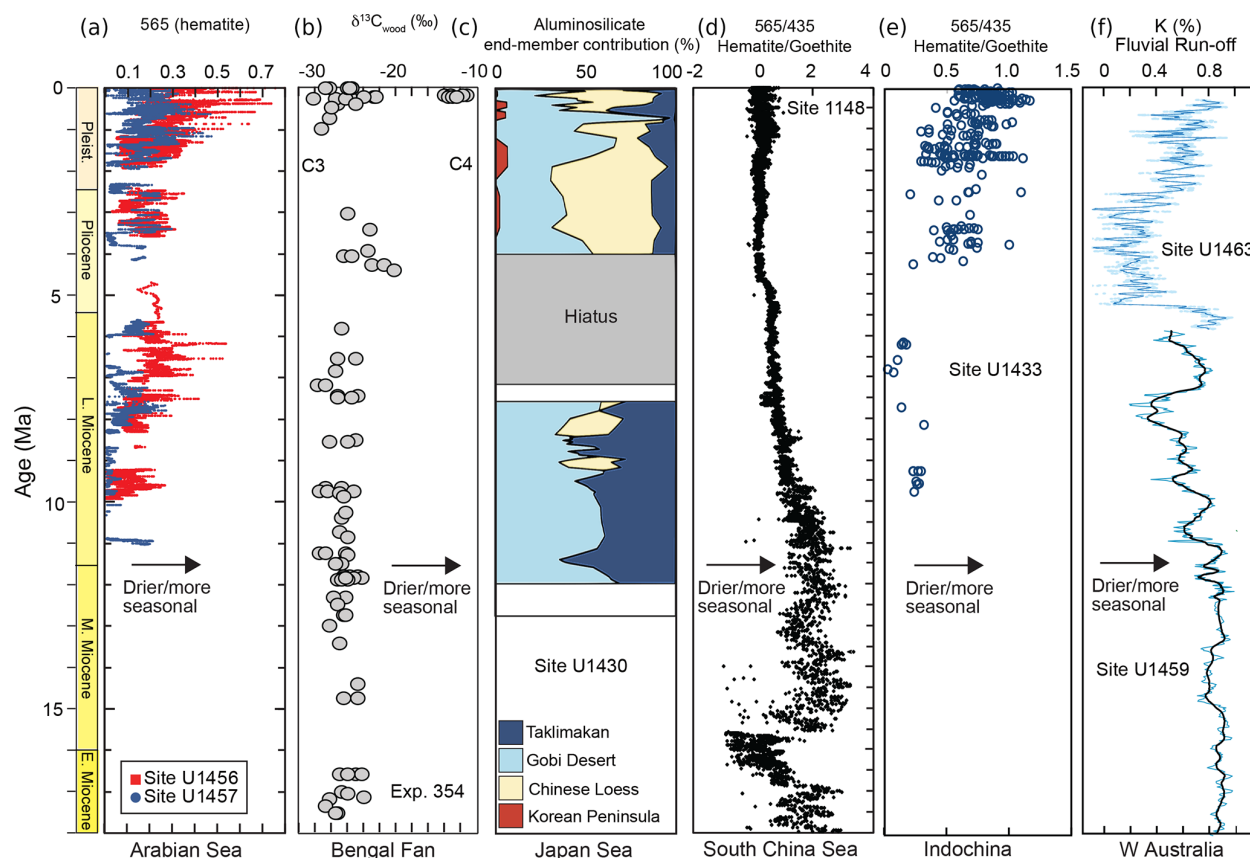
Figure 10. Compilation and comparison of monsoon related proxies from across the Asia–Australia region. **(a)** Hematite content from Laxmi Basin measured by 565 nm spectral analysis (Zhou et al., 2021), **(b)** $\delta^{13}C$ of wood from Bengal fan sediments (data from Lee et al., 2019), **(c)** source of wind-blown sediment in the Sea of Japan (Anderson et al., 2020), **(d)** hematite / goethite relative abundance tracked by 565/435 nm ratio from spectral analysis from northern South China Sea (Clift et al., 2008), **(e)** hematite / goethite relative abundance tracked by 565/435 nm ratio from SW South China Sea (data from Liu et al., 2019) and, **(f)** K (%) contents from western Australia acting a proxy for fluvial run-off at Site U1463 in NW Australia (data from Christensen et al., 2017) and Site U1459 in SW Australia (data from Groeneveld et al., 2017).

areas have seen increasing aridity, southern China appears to have become wetter, possibly due to migration of the ITCZ northwards since the late Miocene (Liu et al., 2019). Drying trends elsewhere are not synchronous. In the Indus Basin of SW Asia, drying started after 10 Ma, although the major change in vegetation to being C_4-dominated after around 7.2–7.4 Ma was not linked to changing rainfall but rather cooling of the Arabian Sea (Feakins et al., 2020). Drying started later, after 5 Ma in former Indochina and especially after 4 Ma in the Ganges Basin, although carbon isotope evidence from the Himalayan foreland basin indicates that eastern parts of the basin have essentially never made the C_3 to C_4 transition (Vögeli et al., 2017).

In central Asia, the Taklimakan Desert formed in the early Miocene (Zheng et al., 2015), but further east desiccation of the Chinese Loess Plateau appears to have occurred most strongly in the Pliocene based on records from the Ulleung Basin (Anderson et al., 2020). This migration in aridity may reflect the progressive northeastward growth of the

Tibetan Plateau, starting in the Eocene (Ji et al., 2017) but with further uplift at 25–16 Ma and after 10 Ma (Wang et al., 2022). Lack of correlation between SAM and EAM is consistent with climate models that tie the SAM more closely with the height of the Himalayan topographic barrier (Boos and Kuang, 2010) when considering tectonic ($> 10^6$ years) timescales, while the EAM is influenced more by the height and extent of the Tibetan Plateau and the WPWP, at least by some studies (Tada et al., 2016). Recent climate models emphasize how the northern expansion of the plateau has increased rainfall in East Asia, especially during the drier winter season (Li et al., 2021), at the same time that northeast Tibet and northern China dried (Jiang et al., 2008; Zhang et al., 2021). In general the topography of Asia, including the Iranian Plateau, and even East Africa, acts to steer moisture inland and to focus precipitation, while the monsoon circulation itself reflects seawater temperature gradients (Acosta and Huber, 2020; Bordoni and Schneider, 2008). Thus, on shorter timescales when orbital processes dominate there is a
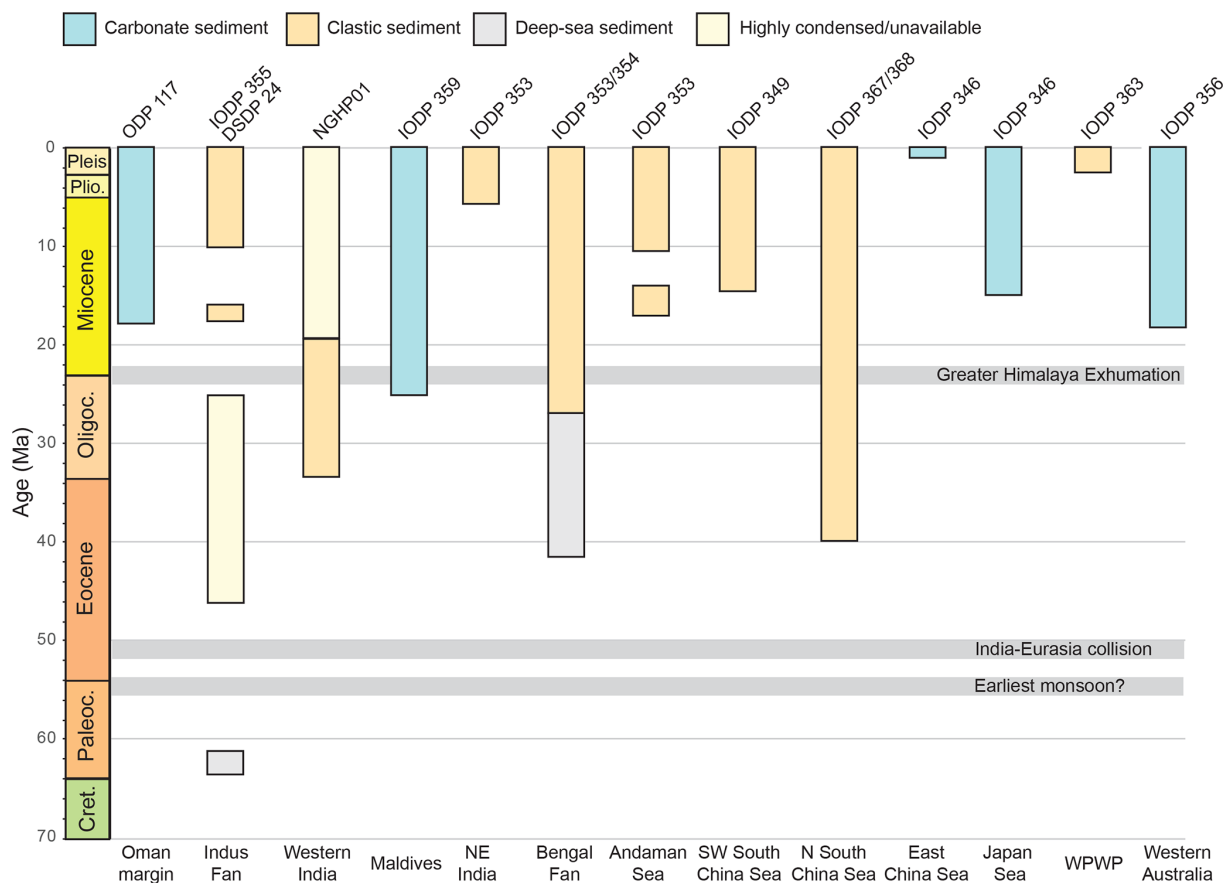
Figure 11. Summary of the temporal coverage now available across the marginal seas of monsoonal Asia, distinguishing between carbonate, biogenic, and oceanic sites and those comprising clastic sediments with records of continental erosion and weathering. Earliest monsoon age is from Licht et al. (2014). India–Eurasia collision age is from Najman et al. (2010). Greater Himalayan exhumation is from Godin et al. (2006).

tendency for the EAM and SAM to wax and wane together, as the surrounding oceans warm and cool.

The weakening monsoon is more generally caused by progressive global cooling since the early Miocene, although the results from the new drilling now indicate that this is not driven by more chemical weathering flux caused by faster erosion in either the western (Clift and Jonell, 2021b) or eastern Himalaya (France-Lanord et al., 2016). Instead, the erosion of areas such as New Guinea under the influence of the Australian monsoon may be critical (Macdonald et al., 2019), adding to the effect of enhanced organic carbon burial (Galy et al., 2007). However, earlier cooling may yet be related to Himalayan uplift in the Eocene–early Miocene. The improved monsoon records clearly show that a simple link between summer rains and topography in Asia is not viable, even assuming the latter can be reconstructed, but must instead involve additional tectonic and climatic processes.

Furthermore, combined records from across the region provide powerful tools for understanding monsoon in a holistic way when combined with onshore records. It is clear that proxies related to oceanographic productivity do not sim-

ply track those of continental rainfall. Monsoon rainfall in South Asia strengthened in the early Miocene (Clift and Webb, 2019), while the upwelling records show monsoon winds starting after 13 Ma (Betzler et al., 2016), linked to the stronger winds of the Somali Jet. This is related to the Iranian and African topographic rise, while Arabian Sea upwelling increased as the Arabian Peninsula became more continental (Sarr et al., 2022). Wind strength and/or stratification of ocean waters are key to controlling biological production but are less important to supplying moisture to inland Asia. Warmer oceans result in greater moisture supply, but the evolving topography diverts this in different directions and focuses precipitation into different areas. While some areas dry, others receive more rainfall, independently of how the oceans evolve. Measuring continental rainfall is not easy and is probably best tracked within limited drainage basins via the evolving vegetation (i.e., C_3 to C_4 balance) coupled with δD measurements. Chemical weathering proxies can play a part but are impacted by both temperature and seasonality, as well as precipitation, so that they must be applied with caution and over limited areas (cf., the contrast-

ing evolution in environments in former Indochina, southern China, and the Chinese Loess Plateau).

10 Future targets

While the monsoon drilling campaign has significantly advanced our understanding of how this climate system has evolved, there remain significant gaps in our comprehension. The almost total lack of Paleogene sedimentary archives is especially noteworthy (Fig. 11). This is a serious shortcoming because few of the marine sections even reach the time of Greater Himalayan exhumation, when monsoon intensification likely happened, let alone the older sections spanning the time of earliest monsoon activity. Climate modeling (Farnsworth et al., 2019) supports sparse terrestrial data (Licht et al., 2014; Sorrel et al., 2017) that indicate the monsoon having initiated in the late Eocene or even earlier, but to date few matching marine records have been cored, although suitable sequences would be accessible in the distal Bengal fan, along the Owen Ridge in the western Arabian Sea, and potentially in the Southwest Indian Margin.

Understanding the evolving continental topography is important when trying to quantify the links between monsoon histories and mountain building in Asia. As part of this effort there has been considerable research done on the evolving river systems of SE Asia which are sensitive to the growth of topography in the eastern Tibetan Plateau. Large-scale drainage capture has been associated with plateau uplift and the re-tilting of east Asia towards the east during the Cenozoic (Wang, 2004). Such studies are hamstrung onshore because of difficulties in constraining sedimentation ages and the lack of long-duration, semi-continuous records. The river systems of SE Asia, especially the Irrawaddy and Mekong, are noteworthy in being central to this debate but with few known sections that record their development studied to date. Drilling in the delta or fan of these systems would help resolve debates about drainage capture while also providing environmental records for SE Asia.

The published and ongoing studies of IODP Expedition 359 Maldive cores show that deposits surrounding carbonate platforms, in particular carbonate drifts, bear a previously underestimated potential for the understanding of the monsoon evolution on million-year timescales but also over shorter intervals and would add substantial knowledge to monsoon fluctuations at all timescales. Potential targets for further research on this topic exist in the Laccadives, the Mascarene Plateau, or the South China Sea platforms.

Author contributions. PDC led the overall writing, wrote the section about the Indus fan, and edited the final paper. CB and GPE wrote the section about the Maldives. SCC, CFL, AH, and WK wrote the sections on the Bay of Bengal and Bengal fan. SW and AH wrote the section on the South China Sea. BC, YR, AH, and SG wrote the sections about the Australian monsoon and western Pacific Warm Pool. RWM and RT wrote the section about the Sea of Japan. All authors contributed to the synthesis and future plans.

References

Abram, N. J., Hargreaves, J. A., Wright, N. M., Thirumalai, K., Ummenhofer, C. C., and England, M. H.: Palaeoclimate perspectives on the Indian Ocean Dipole, Quaternary Sci. Rev., 237, 106302, https://doi.org/10.1016/j.quascirev.2020.106302, 2020.

Acosta, R. P. and Huber, M.: Competing Topographic Mechanisms for the Summer Indo-Asian Monsoon, Geophys. Res. Lett., 47, e2019GL085112, https://doi.org/10.1029/2019GL085112, 2020.

Adhikari, S. K., Sakai, T., and Yoshida, K.: Data report: grain size analysis of Bengal Fan sediments at Sites U1450 and U1451, IODP Expedition 354, Proceedings of the International Ocean Discovery Program, College Station, TX, 354, https://doi.org/10.14379/iodp.proc.354.202.2018, 2018.

Ali, S., Hathorne, E. C., and Frank, M.: Persistent Provenance of South Asian Monsoon-Induced Silicate Weathering Over the Past 27 Million Years, Paleoceanography and Paleoclimatology, 36, e2020PA003909, https://doi.org/10.1029/2020PA003909, 2021.

Allen, M. B. and Armstrong, H. A.: Reconciling the Intertropical Convergence Zone, Himalayan/Tibetan tectonics, and the onset of the Asian monsoon system, J. Asian Earth Sci., 44, 36–47, https://doi.org/10.1016/j.jseaes.2011.04.018, 2012.

Altabet, M. A., Francois, R., Murray, D. W., and Prell, W. L.: Climate-related variations in denitrification in the Arabian Sea from sediment ^{15}N / ^{14}N ratios, Nature, 373, 506–509, 1995.

An, Z., Kutzbach, J. E., Prell, W. L., and Porter, S. C.: Evolution of Asian monsoons and phased uplift of the Himalaya-Tibetan Plateau since late Miocene times, Nature, 411, 62–66, https://doi.org/10.1038/35075035, 2001.

Anderson, C. H., Murray, R. W., Dunlea, A. G., Giosan, L., Kinsley, C. W., McGee, D., and Tada, R.: Aeolian delivery to Ulle-

ung Basin, Korea (Japan Sea), during development of the East Asian Monsoon through the last 12 Ma, Geol. Mag., 157, 806–817, https://doi.org/10.1017/S001675681900013X, 2020.

Ashcroft, L., Gergis, J., and Karoly, D. J.: Long-term stationarity of El Niño–Southern Oscillation teleconnections in southeastern Australia, Clim. Dynam., 46, 2991–3006, https://doi.org/10.1007/s00382-015-2746-3, 2016.

Auer, G., De Vleeschouwer, D., Smith, R. A., Bogus, K., Groeneveld, J., Grunert, P., Castañeda, I. S., Petrick, B., Christensen, B., Fulthorpe, C., Gallagher, S. J., and Henderiks, J.: Timing and Pacing of Indonesian Throughflow Restriction and Its Connection to Late Pliocene Climate Shifts, Paleoceanography and Paleoclimatology, 34, 635–657, https://doi.org/10.1029/2018PA003512, 2019.

Barnet, J. S. K., Harper, D. T., LeVay, L. J., Edgar, K. M., Henehan, M. J., Babila, T. L., Ullmann, C. V., Leng, M. J., Kroon, D., Zachos, J. C., and Littler, K.: Coupled evolution of temperature and carbonate chemistry during the Paleocene–Eocene; new trace element records from the low latitude Indian Ocean, Earth Planet. Sci. Lett., 545, 116414, https://doi.org/10.1016/j.epsl.2020.116414, 2020.

Beasley, C., Kender, S., Giosan, L., Bolton, C. T., Anand, P., Leng, M. J., Nilsson-Kerr, K., Ullmann, C. V., Hesselbo, S. P., and Littler, K.: Evidence of a South Asian Proto-Monsoon During the Oligocene-Miocene Transition, Paleoceanography and Paleoclimatology, 36, e2021PA004278, https://doi.org/10.1029/2021PA004278, 2021.

Bergmann, F., Schwenk, T., Spiess, V., and France-Lanord, C.: Middle to Late Pleistocene Architecture and Stratigraphy of the Lower Bengal Fan—Integrating Multichannel Seismic Data and IODP Expedition 354 Results, Geochem. Geophy. Geosy., 21, e2019GC008702, https://doi.org/10.1029/2019GC008702, 2020.

Betzler, C. and Eberli, G. P.: Miocene start of modern carbonate platforms, Geology, 47, 771–775, https://doi.org/10.1130/g45994.1, 2019.

Betzler, C., Eberli, G. P., Kroon, D., Wright, J. D., Swart, P. K., Nath, B. N., Alvarez-Zarikian, C. A., Alonso-García, M., Bialik, O. M., Blättler, C. L., Guo, J. A., Haffen, S., Horozai, S., Inoue, M., Jovane, L., Lanci, L., Laya, J. C., Mee, A. L. H., Lüdmann, T., Nakakuni, M., Niino, K., Petruny, L. M., Pratiwi, S. D., Reijmer, J. J. G., Reolid, J., Slagle, A. L., Sloss, C. R., Su, X., Yao, Z., and Young, J. R.: The abrupt onset of the modern South Asian Monsoon winds, Sci. Rep., 6, 29838, https://doi.org/10.1038/srep29838, 2016.

Betzler, C., Eberli, G. P., Alvarez Zarikian, C. A., and Expedition 359 Scientists: Maldives Monsoon and Sea Level, International Ocean Discovery Program, College Station, TX, https://doi.org/10.14379/iodp.proc.359.2017, 2017.

Betzler, C., Eberli, G. P., Lüdmann, T., Reolid, J., Kroon, D., Reijmer, J. J. G., Swart, P. K., Wright, J., Young, J. R., Alvarez-Zarikian, C., Alonso-García, M., Bialik, O. M., Blättler, C. L., Guo, J. A., Haffen, S., Horozal, S., Inoue, M., Jovane, L., Lanci, L., Laya, J. C., Hui Mee, A. L., Nakakuni, M., Nath, B. N., Niino, K., Petruny, L. M., Pratiwi, S. D., Slagle, A. L., Sloss, C. R., Su, X., and Yao, Z.: Refinement of Miocene sea level and monsoon events from the sedimentary archive of the Maldives (Indian Ocean), Prog. Earth Planet. Sci., 5, 5, https://doi.org/10.1186/s40645-018-0165-x, 2018.

Blum, M., Rogers, K., Gleason, J., Najman, Y., Cruz, J., and Fox, L.: Allogenic and Autogenic Signals in the Stratigraphic Record of the Deep-Sea Bengal Fan, Sci. Repts., 8, 7973, https://doi.org/10.1038/s41598-018-25819-5, 2018.

Bolton, C. T., Gray, E., Kuhnt, W., Holbourn, A. E., Lübbers, J., Grant, K., Tachikawa, K., Marino, G., Rohling, E. J., Sarr, A.-C., and Andersen, N.: Secular and orbital-scale variability of equatorial Indian Ocean summer monsoon winds during the late Miocene, Clim. Past, 18, 713–738, https://doi.org/10.5194/cp-18-713-2022, 2022.

Boos, W. R. and Kuang, Z.: Dominant control of the South Asian monsoon by orographic insulation versus plateau heating, Nature, 463, 218–222, https://doi.org/10.1038/nature08707, 2010.

Bordoni, S. and Schneider, T.: Monsoons as eddy-mediated regime transitions of the tropical overturning circulations, Nat. Geosci., 1, 515–519, 2008.

Bretschneider, L., Hathorne, E. C., Huang, H., Lübbers, J., Kochhann, K. G. D., Holbourn, A., Kuhnt, W., Thiede, R., Gebregiorgis, D., Giosan, L., and Frank, M.: Provenance and Weathering of Clays Delivered to the Bay of Bengal During the Middle Miocene: Linkages to Tectonics and Monsoonal Climate, Paleoceanography and Paleoclimatology, 36, e2020PA003917, https://doi.org/10.1029/2020PA003917, 2021.

Cai, M., Xu, Z., Clift, P. D., Khim, B.-K., Lim, D., Yu, Z., Kulhanek, D. K., and Li, T.: Long-term history of sediment inputs to the eastern Arabian Sea and its implications for the evolution of the Indian summer monsoon since 3.7 Ma, Geol. Mag., 157, 908–919, https://doi.org/10.1017/S0016756818000857, 2020.

Cai, W., Cowan, T., Briggs, P., and Raupach, M.: Rising temperature depletes soil moisture and exacerbates severe drought conditions across southeast Australia, Geophys. Res. Lett., 36, L21709, https://doi.org/10.1029/2009GL040334, 2009.

Chang, Z. and Zhou, L.: Evidence for provenance change in deep sea sediments of the Bengal Fan: A 7 million year record from IODP U1444A, J. Asian Earth Sci., 186, 104008, https://doi.org/10.1016/j.jseaes.2019.104008, 2019.

Cheng, H., Edwards, R. L., Sinha, A., Spötl, C., Yi, L., Chen, S., Kelly, M., Kathayat, G., Wang, X., Li, X., Kong, X., Wang, Y., Ning, Y., and Zhang, H.: The Asian monsoon over the past 640 000 years and ice age terminations, Nature, 534, 640–646, https://doi.org/10.1038/nature18591, 2016.

Christensen, B. A., Renema, W., Henderiks, J., De Vleeschouwer, D., Groeneveld, J., Castañeda, I. S., Reuning, L., Bogus, K., Auer, G., Ishiwa, T., McHugh, C. M., Gallagher, S. J., and Fulthorpe, C. S.: Indonesian Throughflow drove Australian climate from humid Pliocene to arid Pleistocene, Geophys. Res. Lett., 44, 6914–6925, https://doi.org/10.1002/2017GL072977, 2017.

Clemens, S. C., Kuhnt, W., LeVay, L. J., and Expedition 353 Scientists: Indian Monsoon Rainfall, International Ocean Discovery Program, College Station, TX, https://doi.org/10.14379/iodp.proc.353.2016, 2016.

Clemens, S. C., Holbourn, A., Kubota, Y., Lee, K. E., Liu, Z., Chen, G., Nelson, A., and Fox-Kemper, B.: Precession-band variance missing from East Asian monsoon runoff, Nat. Commun., 9, 3364, https://doi.org/10.1038/s41467-018-05814-0, 2018.

Clemens, S. C., Yamamoto, M., Thirumalai, K., Giosan, L., Richey, J. N., Nilsson-Kerr, K., Rosenthal, Y., Anand, P., and McGrath, S. M.: Remote and local drivers of Pleistocene South Asian summer

monsoon precipitation: A test for future predictions, Sci. Adv., 7, eabg3848, https://doi.org/10.1126/sciadv.abg3848, 2021.

Clift, P., Lee, J. I., Clark, M. K., and Blusztajn, J.: Erosional response of south China to arc rifting and monsoonal strengthening; a record from the South China Sea, Mar. Geol., 184, 207–226, https://doi.org/10.1016/S0025-3227(01)00301-2, 2002.

Clift, P. D. and d'Alpoim Guedes, J.: Monsoon Rains, Great Rivers and the Development of Farming Civilisations in Asia, Cambridge University Press, Cambridge, 339 pp., https://doi.org/10.1017/9781139342889, 2021.

Clift, P. D. and Jonell, T. N.: Monsoon controls on sediment generation and transport: Mass budget and provenance constraints from the Indus River catchment, delta and submarine fan over tectonic and multi-millennial timescales, Earth-Sci. Rev., 220, 103682, https://doi.org/10.1016/j.earscirev.2021.103682, 2021a.

Clift, P. D. and Jonell, T. N.: Himalayan-Tibetan Erosion is not the Cause of Neogene Global Cooling, Geophys. Res. Lett., 48, e2020GL087742, https://doi.org/10.1029/2020GL087742, 2021b.

Clift, P. D. and Webb, A. G.: A history of the Asian monsoon and its interactions with solid Earth tectonics in Cenozoic South Asia, in: Himalayan Tectonics: A Modern Synthesis, edited by: Searle, M. P., and Treloar, P. J., Special Publications, Geological Society, London, 631–652, https://doi.org/10.1144/SP483.1, 2019.

Clift, P. D., Hodges, K., Heslop, D., Hannigan, R., Hoang, L. V., and Calves, G.: Greater Himalayan exhumation triggered by Early Miocene monsoon intensification, Nat. Geosci., 1, 875–880, https://doi.org/10.1038/ngeo351, 2008.

Clift, P. D., Wan, S., and Blusztajn, J.: Reconstructing Chemical Weathering, Physical Erosion and Monsoon Intensity since 25 Ma in the northern South China Sea: A review of competing proxies, Earth-Sci. Rev., 130, 86–102, https://doi.org/10.1016/j.earscirev.2014.01.002, 2014.

Clift, P. D., Kulhanek, D. K., Zhou, P., Bowen, M. G., Vincent, S. M., Lyle, M., and Hahn, A.: Chemical weathering and erosion responses to changing monsoon climate in the Late Miocene of Southwest Asia, Geol. Mag., 157, 939–955, https://doi.org/10.1017/S0016756819000608, 2020.

Cruz, J. W., Wise, S., and Parker, W. C.: Miocene to Recent calcareous nannofossil biostratigraphy in the eastern Bengal Fan (Indian Ocean): Linking turbidites to tectonic activity during the evolution of the Himalayas, Journal of Nannoplankton Research, 39, 15–28, 2021.

Curry, W. B., Ostermann, D. R., Guptha, M. V. S., and Itekkot, V.: Foraminiferal production and monsoonal upwelling in the Arabian Sea; evidence from sediment traps, in: Upwelling systems; evolution since the early Miocene, edited by: Summerhayes, C. P., Prell, W. L., and Emeis, K. C., Special Publication, Geological Society, London, 93–106, https://doi.org/10.1144/GSL.SP.1992.064.01.06, 1992.

Dailey, S. K., Clift, P. D., Kulhanek, D. K., Blusztajn, J., Routledge, C. M., Calvès, G., O'Sullivan, P., Jonell, T. N., Pandey, D. K., Andò, S., Coletti, G., Zhou, P., Li, Y., Neubeck, N. E., Bendle, J. A. P., Bratenkov, S., Griffith, E. M., Gurumurthy, G. P., Hahn, A., Iwai, M., Khim, B.-K., Kumar, A., Kumar, A. G., Liddy, H. M., Lu, H., Lyle, M. W., Mishra, R., Radhakrishna, T., Saraswat, R., Saxena, R., Scardia, G., Sharma, G. K., Singh, A. D., Steinke, S., Suzuki, K., Tauxe, L., Tiwari, M., Xu, Z., and Yu, Z.: Large-scale Mass Wasting on the Miocene Continental Margin of Western India, Geol. Soc. Amer. Bull., 132, 85–112, https://doi.org/10.1130/B35158.1, 2019.

De Vleeschouwer, D., Auer, G., Smith, R., Bogus, K., Christensen, B., Groeneveld, J., Petrick, B., Henderiks, J., Castañeda, I. S., O'Brien, E., Ellinghausen, M., Gallagher, S. J., Fulthorpe, C. S., and Pälike, H.: The amplifying effect of Indonesian Throughflow heat transport on Late Pliocene Southern Hemisphere climate cooling, Earth Planet. Sci. Lett., 500, 15–27, https://doi.org/10.1016/j.epsl.2018.07.035, 2018.

Ding, Z. L., Xiong, S. F., Sun, J. M., Yang, S. L., Gu, Z. Y., and Liu, T. S.: Pedostratigraphy and paleomagnetism of a ∼ 7.0 Ma eolian loess–red clay sequence at Lingtai, Loess Plateau, north-central China and the implications for paleomonsoon evolution, Palaeogeogr. Palaeocl., 152, 49–66, https://doi.org/10.1016/S0031-0182(99)00034-6, 1999.

Dunlea, A. G., Giosan, L., and Huang, Y.: Pliocene expansion of C_4 vegetation in the Core Monsoon Zone on the Indian Peninsula, Clim. Past, 16, 2533–2546, https://doi.org/10.5194/cp-16-2533-2020, 2020.

Farnsworth, A., Lunt, D. J., Robinson, S. A., Valdes, P. J., Roberts, W. H. G., Clift, P. D., Markwick, P., Su, T., Wrobel, N., Bragg, F., Kelland, S.-J., and Pancost, R. D.: Past East Asian monsoon evolution controlled by paleogeography, not CO_2, Sci. Adv., 5, eaax1697, https://doi.org/10.1126/sciadv.aax1697, 2019.

Fasullo, J.: A mechanism for land–ocean contrasts in global monsoon trends in a warming climate, Clim. Dynam., 39, 1137–1147, https://doi.org/10.1007/s00382-011-1270-3, 2012.

Feakins, S. J., Liddy, H. M., Tauxe, L., Galy, V., Feng, X., Tierney, J. E., Miao, Y., and Warny, S.: Miocene C_4 Grassland Expansion as Recorded by the Indus Fan, Paleoceanography and Paleoclimatology, 35, e2020PA003856, https://doi.org/10.1029/2020PA003856, 2020.

France-Lanord, C., Spiess, V., Klaus, A., Schwenk, T., and Expedition 354 Scientists: Bengal Fan, International Ocean Discovery Program, College Station, TX, https://doi.org/10.14379/iodp.proc.354.2016, 2016.

Gai, C., Liu, Q., Roberts, A. P., Chou, Y., Zhao, X., Jiang, Z., and Liu, J.: East Asian monsoon evolution since the late Miocene from the South China Sea, Earth Planet. Sci. Lett., 530, 115960, https://doi.org/10.1016/j.epsl.2019.115960, 2020.

Gallagher, S. J. and deMenocal, P. B.: Finding dry spells in Ocean Sediments, Oceanography, 32, 38–41, https://doi.org/10.5670/oceanog.2019.120, 2019.

Gallagher, S. J., Fulthorpe, C. S., Bogus, K., and Expedition 356 Scientists: Indonesian Throughflow, International Ocean Discovery Program, College Station, TX, https://doi.org/10.14379/iodp.proc.356.2017, 2017.

Gallagher, S. J., Reuning, L., Himmler, T., Henderiks, J., De Vleeschouwer, D., Groeneveld, J., Rastegar Lari, A., Fulthorpe, C. S., Bogus, K., Renema, W., McGregor, H. V., Kominz, M. A., Auer, G., Baranwal, S., Castañeda, S., Christensen, B. A., Franco, D. R., Gurnis, M., Haller, C., He, Y., Ishiwa, T., Iwatani, H., Jatiningrum, R. S., Korpanty, C. A., Lee, E. Y., Levin, E., Mamo, B. L., McHugh, C. M., Petrick, B. F., Potts, D. C., Takayanagi, H., and Zhang, W.: The enigma of rare Quaternary oolites in the Indian and Pacific Oceans: A result of global oceanographic physicochemical conditions or a sampling bias?, Quaternary Sci. Rev., 200, 114–122, https://doi.org/10.1016/j.quascirev.2018.09.028, 2018.

Galy, V., France-Lanord, C., Beyssac, O., Faure, P., Kudrass, H.-R., and Palhol, F.: Efficient organic carbon burial in the Bengal fan sustained by the Himalayan erosional system, Nature, 450, 407–411, https://doi.org/10.1038/nature06273, 2007.

Galy, V., France-Lanord, C., and Lartiges, B.: Loading and fate of particulate organic carbon from the Himalaya to the Ganga–Brahmaputra delta, Geochim. Cosmochim. Acta, 72, 1767–1787, https://doi.org/10.1016/j.gca.2008.01.027, 2008.

Galy, V., France-Lanord, C., Peucker-Ehrenbrink, B., and Huyghe, P.: Sr–Nd–Os evidence for a stable erosion regime in the Himalaya during the past 12 Myr, Earth Planet. Sci. Lett., 290, 474–480, https://doi.org/10.1016/j.epsl.2010.01.004, 2010.

Gebregiorgis, D., Hathorne, E. C., Giosan, L., Clemens, S., Nürnberg, D., and Frank, M.: Southern Hemisphere forcing of South Asian monsoon precipitation over the past $\sim$ 1 million years, Nat. Commun., 9, 4702, https://doi.org/10.1038/s41467-018-07076-2, 2018.

Gentilli, J.: Australian climate patterns, Thomas Nelson, Melbourne, ISBN 0170049048, 1972.

Godin, L., Grujic, D., Law, R. D., and Searle, M. P.: Channel flow, ductile extrusion and exhumation in continental collision zones; an introduction, in: Channel Flow, Ductile Extrusion, and Exhumation of Lower-Middle Crust in Continental Collision Zones, edited by: Law, R. D., Searle, M. P., and Godin, L., Special Publication, Geological Society, London, 1–23, https://doi.org/10.1144/GSL.SP.2006.268.01.01, 2006.

Gordon, A. L.: Oceanography of the Indonesian seas and their throughflow, Oceanography, 18, 14–27, https://doi.org/10.5670/oceanog, 2005.

Groeneveld, J., Henderiks, J., Renema, W., McHugh, C. M., Vleeschouwer, D. D., Christensen, B. A., Fulthorpe, C. S., Reuning, L., Gallagher, S. J., Bogus, K., Auer, G., and Ishiwa, T.: Australian shelf sediments reveal shifts in Miocene Southern Hemisphere westerlies, Sci. Adv., 3, e1602567, https://doi.org/10.1126/sciadv.1602567, 2017.

Gülyüz, E., Durak, H., Özkaptan, M., and Krijgsman, W.: Paleomagnetic constraints on the early Miocene closure of the southern Neo-Tethys (Van region; East Anatolia): Inferences for the timing of Eurasia-Arabia collision, Glob. Planet. Change, 185, 103089, https://doi.org/10.1016/j.gloplacha.2019.103089, 2020.

Gupta, A. K., Yuvaraja, A., Prakasam, M., Clemens, S. C., and Velu, A.: Evolution of the South Asian monsoon wind system since the late Middle Miocene, Palaeogeogr. Palaeocl., 438, 160–167, https://doi.org/10.1016/j.palaeo.2015.08.006, 2015.

Harrison, T. M., Copeland, P., Kidd, W. S. F., and Yin, A.: Raising Tibet, Science, 255, 1663–1670, https://doi.org/10.1126/science.255.5052.1663, 1992.

Hein, C. J., Galy, V., Galy, A., France-Lanord, C., Kudrass, H., and Schwenk, T.: Post-glacial climate forcing of surface processes in the Ganges–Brahmaputra river basin and implications for carbon sequestration, Earth Planet. Sci. Lett., 478, 89–101, https://doi.org/10.1016/j.epsl.2017.08.013, 2017.

Herbert, T. D., Lawrence, K. T., Tzanova, A., Peterson, L. C., Caballero-Gill, R., and Kelly, C. S.: Late Miocene global cooling and the rise of modern ecosystems, Nat. Geosci., 9, 843–847, https://doi.org/10.1038/ngeo2813, 2016.

Herold, N., Huber, M., Greenwood, D. R., Müller, R. D., and Seton, M.: Early to Middle Miocene monsoon climate in Australia, Geology, 39, 3–6, https://doi.org/10.1130/g31208.1, 2011.

Holbourn, A., Kuhnt, W., Clemens, S. C., and Heslop, D.: A $\sim$ 12 Myr Miocene Record of East Asian Monsoon Variability From the South China Sea, Paleoceanography and Paleoclimatology, 36, e2021PA004267, https://doi.org/10.1029/2021PA004267, 2021.

Holbourn, A. E., Kuhnt, W., Clemens, S. C., Kochhann, K. G. D., Jöhnck, J., Lübbers, J., and Andersen, N.: Late Miocene climate cooling and intensification of southeast Asian winter monsoon, Nat. Commun., 9, 1584, https://doi.org/10.1038/s41467-018-03950-1, 2018.

Hovan, S. A. and Rea, D. K.: The Cenozoic Record of Continental Mineral Deposition on Broken and Ninetyeast Ridges, Indian Ocean: Southern African Aridity and Sediment Delivery from the Himalayas, Paleoceanography, 7, 833–860, https://doi.org/10.1029/92PA02176, 1992.

Huang, Y., Clemens, S. C., Liu, W., Wang, Y., and Prell, W. L.: Large-scale hydrological change drove the late Miocene C_4 plant expansion in the Himalayan foreland and Arabian Peninsula, Geology, 35, 531–534, https://doi.org/10.1130/G23666A.1, 2007.

Huyghe, P., Bernet, M., Galy, A., Naylor, M., Cruz, J., Gyawali, B. R., Gemignani, L., and Mugnier, J. L.: Rapid exhumation since at least 13 Ma in the Himalaya recorded by detrital apatite fission-track dating of Bengal fan (IODP Expedition 354) and modern Himalayan river sediments, Earth Planet. Sci. Lett., 534, 116078, https://doi.org/10.1016/j.epsl.2020.116078, 2020.

Irino, T., Tada, R., Ikehara, K., Sagawa, T., Karasuda, A., Kurokawa, S., Seki, A., and Lu, S.: Construction of perfectly continuous records of physical properties for dark-light sediment sequences collected from the Japan Sea during Integrated Ocean Drilling Program Expedition 346 and their potential utilities as paleoceanographic studies, Prog. Earth Planet. Sci., 5, 23, https://doi.org/10.1186/s40645-018-0176-7, 2018.

Ishiwa, T., Yokoyama, Y., Reuning, L., McHugh, C. M., De Vleeschouwer, D., and Gallagher, S. J.: Australian Summer Monsoon variability in the past 14 000 years revealed by IODP Expedition 356 sediments, Prog. Earth Planet. Sci., 6, 17, https://doi.org/10.1186/s40645-019-0262-5, 2019.

Ji, J., Zhang, K., Clift, P. D., Zhuang, G., Song, B., Ke, X., and Xu, Y.: High-resolution magnetostratigraphic study of the Paleogene-Neogene strata in the Northern Qaidam Basin: Implications for the growth of the Northeastern Tibetan Plateau, Gondwana Res., 46, 141–155, https://doi.org/10.1016/j.gr.2017.02.015, 2017.

Jian, Z., Larsen, H. C., Alvarez Zarikian, C. A., and Expedition 368 Scientists: Expedition 368 Preliminary Report: South China Sea Rifted Margin, International Ocean Discovery Program, College Station, TX, https://doi.org/10.14379/iodp.pr.368.2018, 2018.

Jiang, D., Ding, Z., Drange, H., and Gao, Y.: Sensitivity of East Asian climate to the progressive uplift and expansion of the Tibetan Plateau under the mid-Pliocene boundary conditions, Adv. Atmos. Sci., 25, 709–722, https://doi.org/10.1007/s00376-008-0709-x, 2008.

Jiang, H. and Ding, Z.: A 20 Ma pollen record of East-Asian summer monsoon evolution from Guyuan, Ningxia, China, Palaeogeogr. Palaeocl., 265, 30–38, https://doi.org/10.1016/j.palaeo.2008.04.016, 2008.

Jöhnck, J., Kuhnt, W., Holbourn, A., and Andersen, N.: Variability of the Indian Monsoon in the Andaman Sea Across the Miocene-Pliocene Transition, Paleoceanography and Paleoclimatology,

35, e2020PA003923, https://doi.org/10.1029/2020PA003923, 2020.

Joussain, R., Liu, Z., Colin, C., Duchamp-Alphonse, S., Yu, Z., Moréno, E., Fournier, L., Zaragosi, S., Dapoigny, A., Meynadier, L., and Bassinot, F.: Link between Indian monsoon rainfall and physical erosion in the Himalayan system during the Holocene, Geochem. Geophy., Geosy., 18, 3452–3469, https://doi.org/10.1002/2016GC006762, 2017.

Kajtar, J. B., Santoso, A., England, M. H., and Cai, W.: Indo-Pacific Climate Interactions in the Absence of an Indonesian Throughflow, J. Climate, 28, 5017–5029, https://doi.org/10.1175/jcli-d-14-00114.1, 2015.

Karatsolis, B. T., De Vleeschouwer, D., Groeneveld, J., Christensen, B., and Henderiks, J.: The late Miocene to early Pliocene "Humid Interval" on the NW Australian shelf: Disentangling climate forcing from regional basin evolution, Paleoceanography and Paleoclimatology, 35, e2019PA003780, https://doi.org/10.1029/2019PA003780, 2020.

Khim, B.-K., Lee, J., Ha, S., Park, J., Pandey, D. K., Clift, P. D., Kulhanek, D. K., Steinke, S., Griffith, E. M., Suzuki, K., and Xu, Z.: Variations in $\delta13C$ values of sedimentary organic matter since late Miocene time in the Indus Fan (IODP Site 1457) of the eastern Arabian Sea, Geol. Mag., 157, 1012–1021, https://doi.org/10.1017/S0016756818000870, 2020.

Kim, J.-E., Khim, B.-K., Ikehara, M., and Lee, J.: Orbital-scale denitrification changes in the Eastern Arabian Sea during the last 800 kyrs, Sci. Repts., 8, 7027, https://doi.org/10.1038/s41598-018-25415-7, 2018.

Krebs, U., Park, W., and Schneider, B.: Pliocene aridification of Australia caused by tectonically induced weakening of the Indonesian throughflow, Palaeogeogr. Palaeocl., 309, 111–117, https://doi.org/10.1016/j.palaeo.2011.06.002, 2011.

Kroon, D., Steens, T., and Troelstra, S. R.: Onset of Monsoonal related upwelling in the western Arabian Sea as revealed by planktonic foraminifers, in: Proceedings of the Ocean Drilling Program, Scientific Results, edited by: Prell, W., and Niitsuma, N., Ocean Drilling Program, College Station, TX, 257–263, https://doi.org/10.2973/odp.proc.sr.117.126.1991, 1991.

Kubota, Y., Kimoto, K., Tada, R., Uchida, M., and Ikehara, K.: Millennial-scale variability of East Asian summer monsoon inferred from sea surface salinity in the northern East China Sea (ECS) and its impact on the Japan Sea during Marine Isotope Stage (MIS) 3, Prog. Earth Planet. Sci., 6, 39, https://doi.org/10.1186/s40645-019-0283-0, 2019.

Kuhnt, W., Holbourn, A. E., Jöhnck, J., and Lübbers, J.: Miocene to Pleistocene Palaeoceanography of the Andaman Region: Evolution of the Indian Monsoon on a Warmer-Than-Present Earth, in: The Andaman Islands and Adjoining Offshore: Geology, Tectonics and Palaeoclimate, edited by: Ray J., R. M., Society of Earth Scientists Series, Springer, https://doi.org/10.1007/978-3-030-39843-9_13, 2020.

Kunkelova, T., Jung, S. J. A., de Leau, E. S., Odling, N., Thomas, A. L., Betzler, C., Eberli, G. P., Alvarez-Zarikian, C. A., Alonso-García, M., Bialik, O. M., Blättler, C. L., Guo, J. A., Haffen, S., Horozal, S., Mee, A. L. H., Inoue, M., Jovane, L., Lanci, L., Laya, J. C., Lüdmann, T., Bejugam, N. N., Nakakuni, M., Niino, K., Petruny, L. M., Pratiwi, S. D., Reijmer, J. J. G., Reolid, J., Slagle, A. L., Sloss, C. R., Su, X., Swart, P. K., Wright, J. D., Yao, Z., Young, J. R., Lindhorst, S., Stainbank, S., Rueggeberg,

A., Spezzaferri, S., Carrasqueira, I., Yu, S., and Kroon, D.: A two million year record of low-latitude aridity linked to continental weathering from the Maldives, Prog. Earth Planet. Sci., 5, 86, https://doi.org/10.1186/s40645-018-0238-x, 2018.

Kurokawa, S., Tada, R., Matsuzaki, K. M., Irino, T., and Johanna, L.: Cyclostratigraphy of the Late Miocene to Pliocene sediments at IODP sites U1425 and U1430 in the Japan Sea and paleoceanographic implications, Prog. Earth Planet. Sci., 6, 2, https://doi.org/10.1186/s40645-018-0250-1, 2019.

LaRiviere, J. P., Ravelo, A. C., Crimmins, A., Dekens, P. S., Ford, H. L., Lyle, M., and Wara, M. W.: Late Miocene decoupling of oceanic warmth and atmospheric carbon dioxide forcing, Nature, 486, 97–100, https://doi.org/10.1038/nature11200, 2012.

Lau, N.-C. and Wang, B.: Interactions between the Asian monsoon and the El Niño/Southern oscillation, in: The Asian Monsoon, Springer, 479–512, https://doi.org/10.1007/3-540-37722-0_12, 2006.

Lee, H., Galy, V., Feng, X., Ponton, C., Galy, A., France-Lanord, C., and Feakins, S. J.: Sustained wood burial in the Bengal Fan over the last 19 My, P. Natl. Acad. Sci. USA, 116, 22518–22525, https://doi.org/10.1073/pnas.1913714116, 2019.

Lee, J., Kim, S., and Khim, B.-K.: A paleoproductivity shift in the northwestern Bay of Bengal (IODP Site U1445) across the Mid-Pleistocene transition in response to weakening of the Indian summer monsoon, Palaeogeogr. Palaeocl., 560, 110018, https://doi.org/10.1016/j.palaeo.2020.110018, 2020a.

Lee, J., Kim, S., Lee, J. I., Cho, H. G., Phillips, S. C., and Khim, B.-K.: Monsoon-influenced variation of clay mineral compositions and detrital Nd-Sr isotopes in the western Andaman Sea (IODP Site U1447) since the late Miocene, Palaeogeogr. Palaeocl., 538, 109339, https://doi.org/10.1016/j.palaeo.2019.109339, 2020b.

Lenard, S., Cruz, J., France-Lanord, C., and Lavé, J.: Data report: calcareous nannofossils and lithologic constraints on the age model of IODP Site U1450, Expedition 354, Bengal Fan, Proceedings of the International Ocean Discovery Program, College Station, TX, 354, https://doi.org/10.14379/iodp.proc.354.203.2020, 2020a.

Lenard, S. J. P., Lavé, J., France-Lanord, C., Aumaître, G., Bourlès, D. L., and Keddadouche, K.: Steady erosion rates in the Himalayas through late Cenozoic climatic changes, Nature Geosci., 13, 448–452, https://doi.org/10.1038/s41561-020-0585-2, 2020b.

Li, C.-F., Lin, J., Kulhanek, D. K., and Expedition 349 Scientists: South China Sea Tectonics, International Ocean Discovery Program, College Station, TX, https://doi.org/10.14379/iodp.proc.349.102.2015, 2015.

Li, S.-F., Valdes, P. J., Farnsworth, A., Davies-Barnard, T., Su, T., Lunt, D. J., Spicer, R. A., Liu, J., Deng, W.-Y.-D., Huang, J., Tang, H., Ridgwell, A., Chen, L.-L., and Zhou, Z.-K.: Orographic evolution of northern Tibet shaped vegetation and plant diversity in eastern Asia, Sci. Adv., 7, eabc7741, https://doi.org/10.1126/sciadv.abc7741, 2021.

Licht, A., Cappelle, M. v., Abels, H. A., Ladant, J.-B., Trabucho-Alexandre, J., France-Lanord, C., Donnadieu, Y., Vandenberghe, J., Rigaudier, T., Lecuyer, C., Terry, D., Adriaens, R., Boura, A., Guo, Z., Soe, A. N., Quade, J., Dupont-Nivet, G., and Jaeger, J.-J.: Asian monsoons in a late Eocene greenhouse world, Nature, 513, 501–506, https://doi.org/10.1038/nature13704, 2014.

Lindhorst, S., Betzler, C., and Kroon, D.: Wind variability over the northern Indian Ocean during the past 4 million years – Insights from coarse aeolian dust (IODP exp. 359, site U1467, Maldives), Palaeogeogr. Palaeocl., 536, 109371, https://doi.org/10.1016/j.palaeo.2019.109371, 2019.

Ling, A., Eberli, G. P., Swart, P. K., Reolid, J., Stainbank, S., Rüggeberg, A., and Betzler, C.: Middle Miocene platform drowning in the Maldives associated with monsoon-related intensification of currents, Palaeogeogr. Palaeocl., 567, 110275, https://doi.org/10.1016/j.palaeo.2021.110275, 2021.

Liu, C., Clift, P. D., Giosan, L., Miao, Y., Warny, S., and Wan, S.: Paleoclimatic evolution of the SW and NE South China Sea and its relationship with spectral reflectance data over various age scales, Palaeogeogr. Palaeocl., 525, 25–43, https://doi.org/10.1016/j.palaeo.2019.02.019, 2019.

Lübbers, J., Kuhnt, W., Holbourn, A. E., Bolton, C. T., Gray, E., Usui, Y., Kochhann, K. G. D., Beil, S., and Andersen, N.: The Middle to Late Miocene "Carbonate Crash" in the Equatorial Indian Ocean, Paleoceanography and Paleoclimatology, 34, 813–832, https://doi.org/10.1029/2018PA003482, 2019.

Lüdmann, T., Betzler, C., Eberli, G. P., Reolid, J., Reijmer, J. J. G., Sloss, C. R., Bialik, O. M., Alvarez-Zarikian, C. A., Alonso-García, M., Blättler, C. L., Guo, J. A., Haffen, S., Horozal, S., Inoue, M., Jovane, L., Kroon, D., Lanci, L., Laya, J. C., Mee, A. L. H., Nakakuni, M., Nath, B. N., Niino, K., Petruny, L. M., Pratiwi, S. D., Slagle, A. L., Su, X., Swart, P. K., Wright, J. D., Yao, Z., and Young, J. R.: Carbonate delta drift: A new sediment drift type, Mar. Geol., 401, 98–111, https://doi.org/10.1016/j.margeo.2018.04.011, 2018.

Lupker, M., France-Lanord, C., Galy, V., Lave, J., and Kudrass, H.: Increasing chemical weathering in the Himalayan system since the Last Glacial Maximum, Earth Planet. Sci. Lett., 365, 243–252, https://doi.org/10.1016/j.epsl.2013.01.038, 2013.

Macdonald, F. A., Swanson-Hysell, N. L., Park, Y., Lisiecki, L., and Jagoutz, O.: Arc-continent collisions in the tropics set Earth's climate state, Science, 364, 181–184, https://doi.org/10.1126/science.aav5300, 2019.

Madella, M. and Fuller, D. Q.: Palaeoecology and the Harappan Civilisation of South Asia: a reconsideration, Quaternary Sci. Rev., 25, 1283–1301, https://doi.org/10.1016/j.quascirev.2005.10.012, 2006.

Manabe, S. and Terpstra, T. B.: The effects of mountains on the general circulation of the atmosphere as identified by numerical experiments, J. Atmos. Sci., 31, 3–42, https://doi.org/10.1175/1520-0469(1974)031<0003:TEOMOT>2.0.CO;2, 1974.

Matsuzaki, K. M., Suzuki, N., and Tada, R.: An intensified East Asian winter monsoon in the Japan Sea between 7.9 and 6.6 Ma, Geology, 48, 919–923, https://doi.org/10.1130/g47393.1, 2020.

McBride, J. L.: Tropical cyclones in the Southern Hemisphere summer monsoon, Second International Conference on Southern Hemisphere Meteorology, 1–5 December 1986, Wellington, New Zealand, American Meteorological Society, Boston, 358–364, 1986.

McGrath, S. M., Clemens, S. C., Huang, Y., and Yamamoto, M.: Greenhouse Gas and Ice Volume Drive Pleistocene Indian Summer Monsoon Precipitation Isotope Variability, Geophys. Res. Lett., 48, e2020GL092249, https://doi.org/10.1029/2020GL092249, 2021.

McNeill, L. C., Dugan, B., Backman, J., Pickering, K. T., Pouderoux, H. F. A., Henstock, T. J., Petronotis, K. E., Carter, A., Chemale, F., Milliken, K. L., Kutterolf, S., Mukoyoshi, H., Chen, W., Kachovich, S., Mitchison, F. L., Bourlange, S., Colson, T. A., Frederik, M. C. G., Guèrin, G., Hamahashi, M., House, B. M., Hüpers, A., Jeppson, T. N., Kenigsberg, A. R., Kuranaga, M., Nair, N., Owari, S., Shan, Y., Song, I., Torres, M. E., Vannucchi, P., Vrolijk, P. J., Yang, T., Zhao, X., and Thomas, E.: Understanding Himalayan erosion and the significance of the Nicobar Fan, Earth Planet. Sci. Lett., 475, 134–142, https://doi.org/10.1016/j.epsl.2017.07.019, 2017.

Meinicke, N., Reimi, M. A., Ravelo, A. C., and Meckler, A. N.: Coupled Mg / Ca and Clumped Isotope Measurements Indicate Lack of Substantial Mixed Layer Cooling in the Western Pacific Warm Pool During the Last ∼ 5 Million Years, Paleoceanography and Paleoclimatology, 36, e2020PA004115, https://doi.org/10.1029/2020PA004115, 2021.

Miao, Y., Warny, S., Clift, P. D., Liu, C., and Gregory, M.: Evidence of continuous Asian summer monsoon weakening as a response to global cooling over the last 8 Ma, Gondwana Res., 52, 48–58, https://doi.org/10.1016/j.gr.2017.09.003, 2017.

Molnar, P., England, P., and Martinod, J.: Mantle Dynamics, Uplift of the Tibetan Plateau, and the Indian Monsoon, Rev. Geophys., 31, 357–396, https://doi.org/10.1029/93RG02030, 1993.

Molnar, P. H. and Rajagopalan, B.: Late Miocene upward and outward growth of eastern Tibet and decreasing monsoon rainfall over the northwestern Indian subcontinent since ∼ 10 Ma, Geophys. Res. Lett., 39, L09702, https://doi.org/10.1029/2012GL051305, 2012.

Najman, Y., Appel, E., Boudagher-Fadel, M., Bown, P., Carter, A., Garzanti, E., Godin, L., Han, J., Liebke, U., Oliver, G., Parrish, R., and Vezzoli, G.: Timing of India-Asia collision: Geological, biostratigraphic, and palaeomagnetic constraints, J. Geophys. Res., 115, B12416, https://doi.org/10.1029/2010JB007673, 2010.

Najman, Y., Mark, C., Barfod, D. N., Carter, A., Parrish, R., Chew, D., and Gemignani, L.: Spatial and temporal trends in exhumation of the Eastern Himalaya and syntaxis as determined from a multitechnique detrital thermochronological study of the Bengal Fan, GSA Bulletin, 131, 1607–1622, https://doi.org/10.1130/b35031.1, 2019.

Neale, R. and Slingo, J.: The maritime continent and its role in the global climate: A GCM study, J. Climate, 16, 834–848, 2003.

Nilsson-Kerr, K., Anand, P., Sexton, P. F., Leng, M. J., Misra, S., Clemens, S. C., and Hammond, S. J.: Role of Asian summer monsoon subsystems in the inter-hemispheric progression of deglaciation, Nat. Geosci., 12, 290–295, https://doi.org/10.1038/s41561-019-0319-5, 2019.

Nilsson-Kerr, K., Anand, P., Holden, P. B., Clemens, S. C., and Leng, M. J.: Dipole patterns in tropical precipitation were pervasive across landmasses throughout Marine Isotope Stage 5, Communications Earth & Environment, 2, 64, https://doi.org/10.1038/s43247-021-00133-7, 2021.

Pandey, D. K., Clift, P. D., Kulhanek, D. K., and Expedition 355 Scientists: Arabian Sea Monsoon, Proceedings of the International Ocean Discovery Program, College Station TX, 355, https://doi.org/10.14379/iodp.proc.355.2016, 2016.

Pei, R., Kuhnt, W., Holbourn, A., Hingst, J., Koppe, M., Schultz, J., Kopetz, P., Zhang, P., and Andersen, N.:

Monitoring Australian Monsoon variability over the past four glacial cycles, Palaeogeogr. Palaeocl., 568, 110280, https://doi.org/10.1016/j.palaeo.2021.110280, 2021.

Peketi, A., Mazumdar, A., Pillutla, S. P. K., Sawant, B., and Gupta, H.: Climatic and Tectonic Control on the Bengal Fan Sedimentation Since the Pliocene, Geochem. Geophy. Geosy., 22, e2020GC009448, https://doi.org/10.1029/2020GC009448, 2021.

Prell, W. L. and Kutzbach, J. E.: Sensitivity of the Indian Monsoon to forcing parameters and implications for its evolution, Nature, 360, 647–652, https://doi.org/10.1038/360647a0, 1992.

Prell, W. L., Murray, D. W., Clemens, S. C., and Anderson, D. M.: Evolution and variability of the Indian Ocean Summer Monsoon: evidence from the western Arabian Sea drilling program, in: Synthesis of results from scientific drilling in the Indian Ocean, edited by: Duncan, R. A., Rea, D. K., Kidd, R. B., von Rad, U., and Weissel, J. K., Geophysical Monograph, American Geophysical Union, Washington, DC, 447–469, https://doi.org/10.1029/GM070p0447, 1992.

Qiang, X., An, Z., Song, Y., Chang, H., Sun, Y., Liu, W., Ao, H., Dong, J., Fu, C., Wu, F., Lu, F., Cai, Y., Zhou, W., Cao, J., Xu, X., and Ai, L.: New eolian red clay sequence on the western Chinese Loess Plateau linked to onset of Asian desertification about 25 Ma ago, Science China Earth Sciences, 54, 136–144, https://doi.org/10.1007/s11430-010-4126-5, 2011.

Quade, J., Cerling, T. E., and Bowman, J. R.: Development of Asian monsoon revealed by marked ecological shift during the latest Miocene in northern Pakistan, Nature, 342, 163–166, https://doi.org/10.1038/342163a0, 1989.

Ravelo, A. C., Lawrence, K. T., Fedorov, A., and Ford, H. L.: Comment on "A 12-million-year temperature history of the tropical Pacific Ocean", Science, 346, 1467, https://doi.org/10.1126/science.1257618, 2014.

Raymo, M. E. and Ruddiman, W. F.: Tectonic forcing of Late Cenozoic climate, Nature, 359, 117–122, https://doi.org/10.1038/359117a0, 1992.

Reichart, G. J., Lourens, L. J., and Zachariasse, W. J.: Temporal variability in the northern Arabian Sea oxygen minimum zone (OMZ) during the last 225 000 years, Paleoceanography, 13, 607–621, https://doi.org/10.1029/98PA02203, 1998.

Reilly, B. T., Bergmann, F., Weber, M. E., Stoner, J. S., Selkin, P., Meynadier, L., Schwenk, T., Spiess, V., and France-Lanord, C.: Middle to Late Pleistocene Evolution of the Bengal Fan: Integrating Core and Seismic Observations for Chronostratigraphic Modeling of the IODP Expedition 354 8° North Transect, Geochem. Geophy. Geosy., 21, e2019GC008878, https://doi.org/10.1029/2019GC008878, 2020.

Reolid, J., Betzler, C., and Lüdmann, T.: The record of Oligocene – Middle Miocene paleoenvironmental changes in a carbonate platform (IODP Exp. 359, Maldives, Indian Ocean), Mar. Geol., 412, 199–216, https://doi.org/10.1016/j.margeo.2019.03.011, 2019.

Reolid, J., Betzler, C., Braga, J. C., Lüdmann, T., Ling, A., and Eberli, G. P.: Facies and geometry of drowning steps in a Miocene carbonate platform (Maldives), Palaeogeogr. Palaeocl., 538, 109455, https://doi.org/10.1016/j.palaeo.2019.109455, 2020.

Robinson, M., Bartol, M., Bolton, C., Ding, X., Gariboldi, K., Romero, O., and Scientific Party: Biostratigraphic summary,

in: Proceedings of the International Ocean Discovery Program edited by: Clemens, S. C., Kuhnt, W., and LeVay, L. J., International Ocean Discovery Program, College Station, Texas, https://doi.org/10.14379/iodp.proc.353.109.2016, 2016.

Rosenthal, Y., Holbourn, A. E., Kulhanek, D. K., and Expedition 363 Scientists: Western Pacific Warm Pool, International Ocean Discovery Program, College Station, TX, https://doi.org/10.14379/iodp.proc.363.2018, 2018.

Routledge, C. M., Kulhanek, D. K., Tauxe, L., Scardia, G., Singh, A. D., Steinke, S., Griffith, E. M., and Saraswat, R.: Revised geological timescale for IODP Sites U1456 and U1457, Geol. Mag., 157, 961–978, https://doi.org/10.1017/S0016756819000104, 2020.

Sarathchandraprasad, T., Tiwari, M., and Behera, P.: South Asian Summer Monsoon precipitation variability during late Pliocene: Role of Indonesian Throughflow, Palaeogeogr. Palaeocl., 574, 110447, https://doi.org/10.1016/j.palaeo.2021.110447, 2021.

Sarr, A.-C., Donnadieu, Y., Bolton, C. T., Ladant, J.-B., Licht, A., Fluteau, F., Laugié, M., Tardif, D., and Dupont-Nivet, G.: Neogene South Asian monsoon rainfall and wind histories diverged due to topographic effects, Nat. Geosci., 15, 314–319, https://doi.org/10.1038/s41561-022-00919-0, 2022.

Schwenk, T. and Spieß, V.: Architecture and stratigraphy of the Bengal Fan as response to tectonic and climate revealed from high-resolution seismic data, External Controls on Deep-Water Depositional Systems, Special Publication-SEPM (Society of Sedimentary Geologists), 92, 107–131, https://doi.org/10.2110/sepmsp.092.107, 2009.

Seki, A., Tada, R., Kurokawa, S., and Murayama, M.: High-resolution Quaternary record of marine organic carbon content in the hemipelagic sediments of the Japan Sea from bromine counts measured by XRF core scanner, Prog. Earth Planet. Sci., 6, 1, https://doi.org/10.1186/s40645-018-0244-z, 2019.

Shen, X., Wan, S., Colin, C., Tada, R., Shi, X., Pei, W., Tan, Y., Jiang, X., and Li, A.: Increased seasonality and aridity drove the C_4 plant expansion in Central Asia since the Miocene–Pliocene boundary, Earth Planet. Sci. Lett., 502, 74–83, https://doi.org/10.1016/j.epsl.2018.08.056, 2018.

Smith, R. A., Castañeda, I. S., Groeneveld, J., De Vleeschouwer, D., Henderiks, J., Christensen, B. A., Renema, W., Auer, G., Bogus, K., Gallagher, S. J., and Fulthorpe, C. S.: Plio-Pleistocene Indonesian Throughflow Variability Drove Eastern Indian Ocean Sea Surface Temperatures, Paleoceanography and Paleoclimatology, 35, e2020PA003872, https://doi.org/10.1029/2020PA003872, 2020.

Sorrel, P., Eymard, I., Leloup, P.-H., Maheo, G., Olivier, N., Sterb, M., Gourbet, L., Wang, G., Jing, W., Lu, H., Li, H., Yadong, X., Zhang, K., Cao, K., Chevalier, M.-L., and Replumaz, A.: Wet tropical climate in SE Tibet during the Late Eocene, Sci. Rep., 7, 7809, https://doi.org/10.1038/s41598-017-07766-9, 2017.

Sprintall, J., Gordon, A. L., Koch-Larrouy, A., Lee, T., Potemra, J. T., Pujiana, K., and Wijffels, S. E.: The Indonesian seas and their role in the coupled ocean–climate system, Nat. Geosci., 7, 487–492, https://doi.org/10.1038/ngeo2188, 2014.

Steinke, S., Groeneveld, J., Johnstone, H., and Rendle-Bühring, R.: East Asian summer monsoon weakening after 7.5 Ma: Evidence from combined planktonic foraminifera Mg / Ca and $\delta 18O$ (ODP Site 1146; northern South China Sea), Palaeogeogr. Palaeocl., 289, 33–43, https://doi.org/10.1016/j.palaeo.2010.02.007, 2010.

Sun, X. and Wang, P.: How old is the Asian monsoon system? Palaeobotanical records from China, Palaeogeogr. Palaeocl., 222, 181–222, https://doi.org/10.1016/j.palaeo.2005.03.005, 2005.

Sun, Z., Jian, Z., Stock, J. M., Larsen, H. C., Klaus, A., Alvarez Zarikian, C. A., and Expedition 367/368 Scientists: South China Sea Rifted Margin, International Ocean Discovery Program, College Station, TX https://doi.org/10.14379/iodp.proc.367368.2018, 2018.

Suppiah, R.: The Australian summer monsoon: a review, Prog. Phys. Geog., 16, 283–318, https://doi.org/10.1177/030913339201600302, 1992.

Suzuki, K., Yamamoto, M., and Seki, O.: Late Miocene changes in C_3, C_4 and aquatic plant vegetation in the Indus River basin: evidence from leaf wax $\delta13C$ from Indus Fan sediments, Geol. Mag., 157, 979–988, https://doi.org/10.1017/S0016756819001109, 2020.

Tada, R. and Murray, R. W.: Preface for the article collection "Land–Ocean Linkages under the Influence of the Asian Monsoon", Prog. Earth Planet. Sci., 3, 24, https://doi.org/10.1186/s40645-016-0100-y, 2016.

Tada, R., Irino, T., and Koizumi, I.: Land-ocean linkages over orbital and millennial timescales recorded in late Quaternary sediments of the Japan Sea, Paleoceanography, 14, 236–247, 1999.

Tada, R., Murray, R. W., Alvarez Zarikian, C. A., and Expedition 346 Scientists: Asian Monsoon: onset and evolution of millennial-scale variability of Asian Monsoon and its possible relation with Himalaya and Tibetan plateau, Integrated Ocean Drilling Program, College Station, TX, https://doi.org/10.2204/iodp.proc.346.2015, 2015.

Tada, R., Zheng, H., and Clift, P. D.: Evolution and variability of the Asian monsoon and its potential linkage with uplift of the Himalaya and Tibetan Plateau, Prog. Earth Planet. Sci., 3, 1–26, https://doi.org/10.1186/s40645-016-0080-y, 2016.

Tada, R., Irino, T., Ikehara, K., Karasuda, A., Sugisaki, S., Xuan, C., Sagawa, T., Itaki, T., Kubota, Y., Lu, S., Seki, A., Murray, R. W., Alvarez-Zarikian, C., Anderson, W. T., Bassetti, M.-A., Brace, B. J., Clemens, S. C., da Costa Gurgel, M. H., Dickens, G. R., Dunlea, A. G., Gallagher, S. J., Giosan, L., Henderson, A. C. G., Holbourn, A. E., Kinsley, C. W., Lee, G. S., Lee, K. E., Lofi, J., Lopes, C. I. C. D., Saavedra-Pellitero, M., Peterson, L. C., Singh, R. K., Toucanne, S., Wan, S., Zheng, H., and Ziegler, M.: High-resolution and high-precision correlation of dark and light layers in the Quaternary hemipelagic sediments of the Japan Sea recovered during IODP Expedition 346, Prog. Earth Planet. Sci., 5, 19, https://doi.org/10.1186/s40645-018-0167-8, 2018.

Tagliaro, G., Fulthorpe, C. S., Gallagher, S. J., McHugh, C. M., Kominz, M., and Lavier, L. L.: Neogene siliciclastic deposition and climate variability on a carbonate margin: Australian Northwest Shelf, Mar. Geol., 403, 285–300, https://doi.org/10.1016/j.margeo.2018.06.007, 2018.

Thiry, M.: Palaeoclimatic interpretation of clay minerals in marine deposits; an outlook from the continental origin, Earth-Sci. Rev., 49, 201–221, https://doi.org/10.1016/S0012-8252(99)00054-9, 2000.

Torfstein, A. and Steinberg, J.: The Oligo–Miocene closure of the Tethys Ocean and evolution of the proto-Mediterranean Sea, Sci. Rep., 10, 13817, https://doi.org/10.1038/s41598-020-70652-4, 2020.

Tripathi, S., Tiwari, M., Lee, J., Khim, B.-K., and IODP Expedition 355 Scientists: First evidence of denitrification visà-vis monsoon in the Arabian Sea since Late Miocene, Sci. Rep., 7, 43056, https://doi.org/10.1038/srep43056, 2017.

Vail, P. R., Mitchum, R. M., Todd, R. G., Widmier, J. M., Thompson, S. I., Sangree, J. B., Bubb, J. N., and Hatlelid, W. G.: Seismic stratigraphy and global changes of sealevel, in: Seismic Stratigraphy–Applications to Hydrocarbon Exploration, edited by: Payton, C. E., Memoir, American Association of Petroleum Geologists, Tulsa, OK, 49–212, https://doi.org/10.1306/M26490C3, 1977.

van Ufford, A. Q. and Cloos, M.: Cenozoic tectonics of New Guinea, AAPG Bull., 89, 119–140, https://doi.org/10.1306/08300403073, 2005.

Vögeli, N., Najman, Y., van der Beek, P., Huyghe, P., Wynn, P. M., Govin, G., Veen, I. v. d., and Sachse, D.: Lateral variations in vegetation in the Himalaya since the Miocene and implications for climate evolution, Earth Planet. Sci. Lett., 471, 1–9, https://doi.org/10.1016/j.epsl.2017.04.037, 2017.

Wan, S., Li, A., Clift, P. D., and Stuut, J.-B. W.: Development of the East Asian monsoon: Mineralogical and sedimentologic records in the northern South China Sea since 20 Ma, Palaeogeogr. Palaeocl., 254, 561–582, https://doi.org/10.1016/j.palaeo.2007.07.009, 2007.

Wan, S., Clift, P. D., Li, A., Li, T., and Yin, X.: Geochemical records in the South China Sea: implications for East Asian summer monsoon evolution over the last 20 Ma, in: Monsoon Evolution and Tectonics–Climate Linkage in Asia, edited by: Clift, P. D., Tada, R., and Zheng, H., Special Publication, Geological Society, London, 245–263, https://doi.org/10.1144/SP342.14, 2010.

Wang, B. (Ed.): The Asian Monsoon, Springer-Verlag, Berlin, 795 pp., https://doi.org/10.1007/3-540-37722-0, 2006.

Wang, B., Liu, J., Kim, H.-J., Webster, P. J., Yim, S.-Y., and Xiang, B.: Northern Hemisphere summer monsoon intensified by mega-El Niino/southern oscillation and Atlantic multidecadal oscillation, P. Natl. Acad. Sci. USA, 110, 5347–5352, https://doi.org/10.1073/pnas.1219405110, 2013.

Wang, H. and Mehta, V. M.: Decadal variability of the Indo-Pacific warm pool and its association with atmospheric and oceanic variability in the NCEP-NCAR and SODA reanalyses, J. Climate, 21, 5545–5565, 2008.

Wang, P.: Cenozoic deformation and the history of sealand interactions in Asia, in: Continent-Ocean Interactions in the East Asian Marginal Seas, edited by: Clift, P., Wang, P., Kuhnt, W., and Hayes, D., American Geophysical Union, Washington, DC, 1–22, https://doi.org/10.1029/149GM01, 2004.

Wang, P., Prell, W. L., Blum, P., Arnold, E. M., Buehring, C. J., Chen, M.-P., Clemens, S. C., Clift, P. D., Colin, C. J. G., Farrell, J. W., Higginson, M. J., Jian, Z., Kuhnt, W., Laj, C. E., Lauer-Leredde, C., Leventhal, J. S., Li, A., Li, Q., Lin, J., McIntyre, K., Miranda, C. R., Nathan, S. A., Shyu, J.-P., Solheid, P. A., Su, X., Tamburini, F., Trentesaux, A., Wang, L., Wang, P., Prell, W. L., Blum, P., Arnold, E. M., Buehring, C. J., Chen, M.-P., Clemens, S. C., Clift, P. D., Colin, C. J. G., Farrell, J. W., Higginson, M. J., Jian, Z., Kuhnt, W., Laj, C. E., Lauer-Leredde, C., Leventhal, J. S., Li, A., Li, Q., Lin, J., McIntyre, K., Miranda, C. R., Nathan, S. A., Shyu, J.-P., Solheid, P. A., Su, X., Tamburini, F., Trentesaux, A., and Wang, L.: Leg 184, Ocean Drilling Program, College

Station, TX, Proc. Ocean Drill. Prog., Pt A: Init. Rpt., 184, 1–77, https://doi.org/10.2973/odp.proc.ir.184.2000, 2000.

Wang, W., Zhang, P., Garzione, C. N., Liu, C., Zhang, Z., Pang, J., Wang, Y., Zheng, D., Zheng, W., and Zhang, H.: Pulsed rise and growth of the Tibetan Plateau to its northern margin since ca. 30 Ma, P. Natl. Acad. Sci. USA, 119, e2120364119, https://doi.org/10.1073/pnas.2120364119, 2022.

Weber, M. E., Lantzsch, H., Dekens, P., Das, S. K., Reilly, B. T., Martos, Y. M., Meyer-Jacob, C., Agrahari, S., Ekblad, A., Titschack, J., Holmes, B., and Wolfgramm, P.: 200 000 years of monsoonal history recorded on the lower Bengal Fan - strong response to insolation forcing, Glob. Planet. Change, 166, 107–119, https://doi.org/10.1016/j.gloplacha.2018.04.003, 2018.

Webster, P. J., Magaña, V. O., Palmer, T. N., Shukla, J., Tomas, R. A., Yanai, M., and Yasunari, T.: Monsoons: Processes, predictability, and the prospects for prediction, J. Geophys. Res., 103, 14451–14510, https://doi.org/10.1029/97JC02719, 1998.

Wei, G., Li, X.-H., Liu, Y., Shao, L., and Liang, X.: Geochemical record of chemical weathering and monsoon climate change since the early Miocene in the South China Sea, Paleoceanography, 21, PA4214, https://doi.org/10.1029/2006PA001300, 2006.

Westerhold, T., Marwan, N., Drury, A. J., Liebrand, D., Agnini, C., Anagnostou, E., Barnet, J. S. K., Bohaty, S. M., De Vleeschouwer, D., Florindo, F., Frederichs, T., Hodell, D. A., Holbourn, A. E., Kroon, D., Lauretano, V., Littler, K., Lourens, L. J., Lyle, M., Pälike, H., Röhl, U., Tian, J., Wilkens, R. H., Wilson, P. A., and Zachos, J. C.: An astronomically dated record of Earth's climate and its predictability over the last 66 million years, Science, 369, 1383–1387, https://doi.org/10.1126/science.aba6853, 2020.

Whipple, K. X.: The influence of climate on the tectonic evolution of mountain belts, Nat. Geosci., 2, 1–8, https://doi.org/10.1038/ngeo413, 2009.

Yan, Y. Y.: Intertropical Convergence Zone (ITCZ), in: Encyclopedia of World Climatology, edited by: Oliver, J. E., Springer Netherlands, Dordrecht, 429–432, https://doi.org/10.1007/1-4020-3266-8_110, 2005.

Yang, C., Dang, H., Zhou, X., Zhang, H., Wang, X., Wang, Y., Qiao, P., Jiang, X., and Jian, Z.: Upper ocean hydrographic changes in response to the evolution of the East Asian monsoon in the northern South China Sea during the middle to late Miocene, Glob. Planet. Change, 201, 103478, https://doi.org/10.1016/j.gloplacha.2021.103478, 2021.

Yang, X., Groeneveld, J., Jian, Z., Steinke, S., and Giosan, L.: Middle Miocene Intensification of South Asian Monsoonal Rainfall, Paleoceanography and Paleoclimatology, 35, e2020PA003853, https://doi.org/10.1029/2020PA003853, 2020.

Yoshida, K., Nakajima, T., Matsumoto, Y., Osaki, A., Rai, L. K., Cruz, J. W., and Sakai, H.: Miocene provenance change in Himalayan foreland basin and Bengal Fan sediments, with special reference to detrital garnet chemistry, Island Arc, 30, e12408, https://doi.org/10.1111/iar.12408, 2021.

Zachos, J. C., Dickens, G. R., and Zeebe, R. E.: An early Cenozoic perspective on greenhouse warming and carbon-cycle dynamics, Nature, 451, 279–283, https://doi.org/10.1038/nature06588, 2008.

Zhang, P., Xu, J., Holbourn, A., Kuhnt, W., Beil, S., Li, T., Xiong, Z., Dang, H., Yan, H., Pei, R., Ran, Y., and Wu, H.: Indo-Pacific Hydroclimate in Response to Changes of the Intertropical Convergence Zone: Discrepancy on Precession and Obliquity Bands Over the Last 410 kyr, J. Geophys. Res.-Atmos., 125, e2019JD032125, https://doi.org/10.1029/2019JD032125, 2020.

Zhang, R., Jiang, D., Zhang, Z., and Zhang, C.: Effects of Tibetan Plateau Growth, Paratethys Sea Retreat and Global Cooling on the East Asian Climate by the Early Miocene, Geochem. Geophy. Geosy., 22, e2021GC009655, https://doi.org/10.1029/2021GC009655, 2021.

Zhang, Y. G., Pagani, M., and Liu, Z.: Response to Comment on "A 12-million-year temperature history of the tropical Pacific Ocean", Science, 346, 1467, https://doi.org/10.1126/science.1257930, 2014a.

Zhang, Y. G., Pagani, M., and Liu, Z.: A 12-Million-Year Temperature History of the Tropical Pacific Ocean, Science, 344, 84–87, https://doi.org/10.1126/science.1246172, 2014b.

Zhao, H., Qiang, X., Xu, X., and Sun, Y.: Iron oxide characteristics of the Chinese loess-red clay sequences and their implications for the evolution of the East Asian summer monsoon since the Late Oligocene, Palaeogeogr. Palaeocl., 543, 109604, https://doi.org/10.1016/j.palaeo.2020.109604, 2020.

Zheng, H., Wei, X., Tada, R., Clift, P. D., Wang, B., Jourdan, F., Wang, P., and He, M.: Late Oligocene–early Miocene birth of the Taklimakan Desert, P. Natl. Acad. Sci. USA, 112, 7662–7667, https://doi.org/10.1073/pnas.1424487112, 2015.

Zhou, P., Ireland, T., Murray, R. W., and Clift, P. D.: Marine Sedimentary Records of Chemical Weathering Evolution in the Western Himalaya since 17 Ma, Geosphere, 17, 824–853, https://doi.org/10.1130/GES02211.1, 2021.